Inhibition of Plasmin Generation in Plasma by Heparin, Low Molecular Weight Heparin

and a Covalent Antithrombin-Heparin Complex (ATH)

Gabriela Chang, H. BSc

A Thesis

Submitted to the School of Graduate Studies

In Partial Fulfillment of the Requirements for the Degree

Master of Science

McMaster University

Master of Science (2015)   McMaster University

(Medical Sciences)   Hamilton, ON

TITLE: Inhibition of Plasmin Generation in Plasma by Heparin, Low Molecular Weight Heparin

and a Covalent Antithrombin-Heparin Complex (ATH)

AUTHOR: Gabriela Chang

SUPERVISOR: Dr. Anthony Chan

NUMBER OF PAGES: 104

Abstract

Unfractionated heparin (UFH) and low molecular weight heparin (LMWH) are commonly used anticoagulants to treat thrombotic diseases. However, these anticoagulants are associated with some limitations such as increased bleeding, variable dose response, and the necessity for frequent monitoring. This led to the development of the antithrombin-heparin covalent complex (ATH) which has been shown to overcome many of these limitations. Numerous past studies have proven ATH to be a better anticoagulant in comparison to UFH. More recent studies aimed at studying its interaction with the fibrinolytic pathway. It was observed that ATH inhibited free and fibrin bound plasmin (Pn), the main serine protease of fibrinolysis. As well, the rates of Pn generation on fibrin clots decreased in the presence of ATH. These studies were conducted in purified systems and did not elucidate the interaction of ATH with Pn in the presence of its natural inhibitors, α_2-macroglobulin (α_2-M) and α_2-antiplasmin (α_2-AP). Thus, this study focuses on analyzing the effects of ATH in comparison to UFH and LMWH on Pn generation in plasma, to allow for a better understanding of such mechanisms under more physiological conditions. In comparison to the absence of anticoagulants, total Pn generated decreased in the presence of 0.7 U/ml of UFH or ATH and 2.1 U/ml of ATH. This confirms previous *in vitro* studies in which UFH + AT and ATH can inhibit Pn activity. In addition, quantified Pn bound α_2-M complexes showed a reduction at 0.7 U/ml of ATH suggesting that ATH may be able to compete with α_2-M for Pn. However, the amount of quantified Pn bound α_2-AP complexes were not affected as α_2-AP is a much faster inhibitor of Pn. It was noted that LMWH did not affect Pn generation. As a result, this study adds to our understanding of ATH mechanisms of action and aids in its development for clinical use.

Acknowledgements

I would like to thank my supervisor Dr. Anthony Chan for providing the opportunity to conduct research under his expertise. I greatly appreciate the endless support and life lessons that have been given to me throughout the years of being a part of this research team. I would also like to express my gratitude to Helen Atkinson and Leslie Berry for always going above and beyond to provide advice and guidance. In addition, I would like to thank Dr. Howard Chan for all the invaluable guidance on my research and future career. Lastly, I am thankful to Dr. Paul Kim for agreeing to be on my committee and providing unlimited advice on my research.

Table of Contents

List of Figures

List of Abbreviations

AT	Antithrombin
AT + UFH	Mixtures of non-covalently bound antithrombin and heparin
ATH	Covalent antithrombin-heparin complex
Fib	Cyanogen bromide digested fibrinogen fragments
H	Heparin
HBS	Hepes buffer saline with albumin
II	Prothrombin
IIa	Thrombin
IXa	Activated Factor IX
k_2	Second-order rate constant
LMWH	Low molecular weight heparin
MW	Molecular weight
NPP	Normal human pooled plasma
PBS	Phosphate buffer saline
PES	Phosphate ethylenediaminetetraacetic acid saline buffer
PAI-1	Plasminogen activator inhibitor 1
PAP	Plasmin α_2-Antiplasmin complex
PAT	Plasmin-Antithrombin complex
PATH	Plasmin-ATH complex
Pg	Plasminogen

PgdP	Plasminogen deficient plasma
PAM	Plasmin α_2-Macroglobulin complex
Pn	Plasmin
RCL	Reactive centre loop
SBTI	Soybean trypsin inhibitor
serpin	Serine protease inhibitor
TAFI	Thrombin activatable fibrinolysis inhibitor
TF	Tissue factor
tPA	Tissue plasminogen activator
TSP	Tris saline buffer with polyethylene glycol
UFH	Unfractionated heparin
uPA	Urokinase plasminogen activator
Va	Activated Factor V
VIIa	Activated Factor VII
VIIIa	Activated Factor VIII
vWF	von Willebrand factor
Xa	Activated Factor X
XIa	Activated Factor XI
XIIa	Activated Factor XII
α_2-AP	α_2-Antiplasmin
α_2-M	α_2-Macroglobulin

1 Introduction

Hemostasis is a process that leads to the termination of bleeding in injured blood vessels (1). It involves the balance of several mechanisms including platelets, coagulation, and fibrinolysis in order to prevent bleeding and maintain vascular fluidity (2). An imbalance in these mechanisms, can often lead to embolism, increased bleeding, or thrombosis (2,3). One of the most common therapeutic approaches to treating such imbalances, specifically thrombosis, is the administration of heparin (4). Heparin and its derivatives potentiate antithrombin inhibition of factor Xa, thrombin and other coagulation factors, thus greatly increasing antithrombin's anticoagulant abilities (1,4). However, heparin therapy has its limitations such as limited bioavailability, unwanted protein interactions, and increased bleeding (1,4). In efforts to remove such limitations Chan et al. produced a novel anticoagulant, antithrombin-heparin covalent complex (ATH), that has been shown to have improved anticoagulant abilities (5-8). Along with ATH's ability to inhibit coagulation, previous *in vitro* studies, in purified systems, have suggested that heparin catalyzed AT and ATH can inhibit plasmin, the main serine protease in fibrinolysis (9). Therefore, this study focuses on analyzing the effects of heparin and ATH on plasmin generation in plasma, to allow for a better understanding of such mechanisms under more physiological conditions.
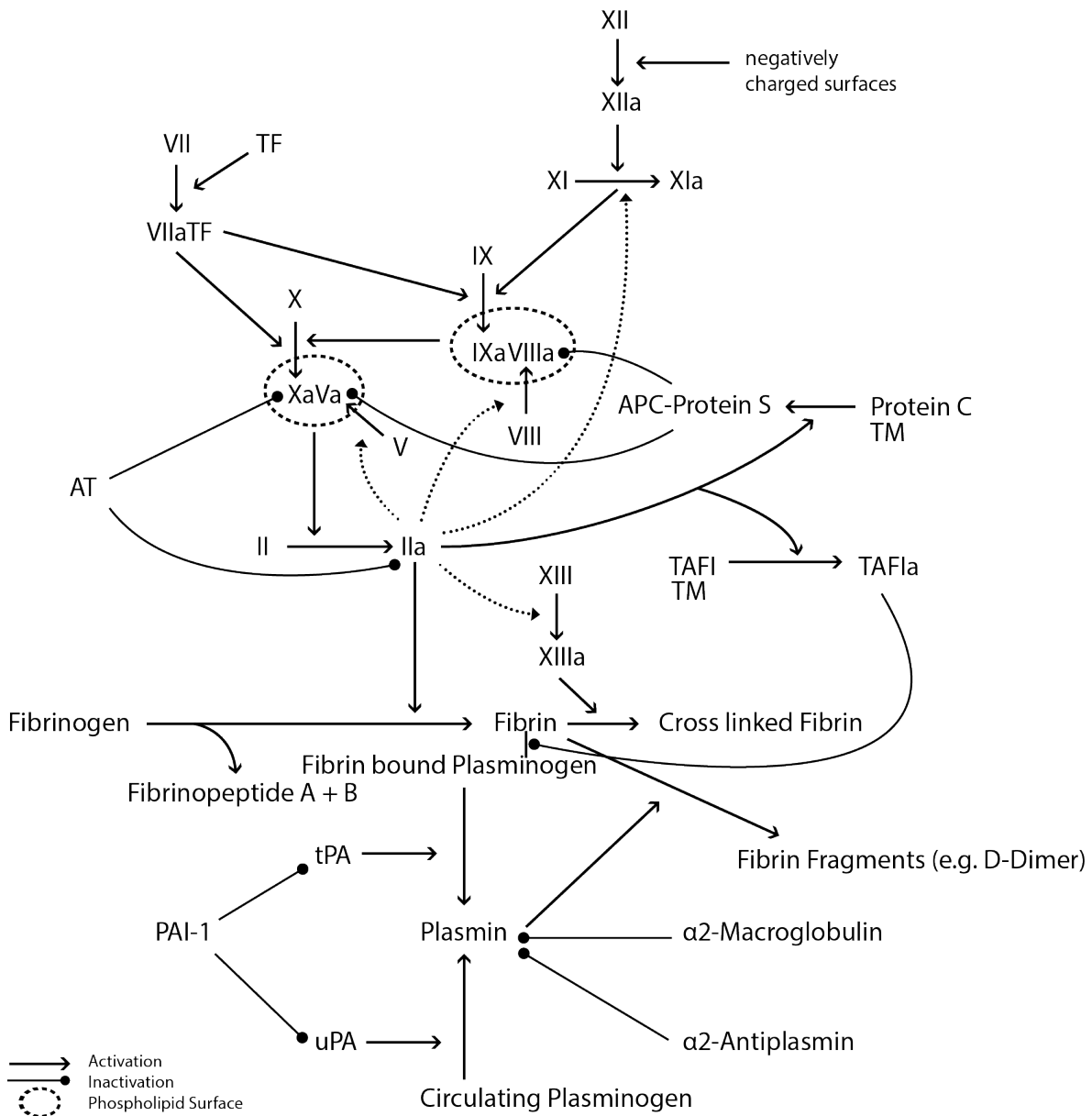
Figure 1. Interaction of Coagulation and Fibrinolysis.

Coagulation Factors are in roman numerals. Activated forms are indicated by the letter 'a'. TF: tissue factor, AT: antithrombin, tPA: tissue-type plasminogen activator, uPA: urokinase-type plasminogen activator, PAI-1: plasminogen activator inhibitor 1, TAFI: thrombin activatable fibrinolysis inhibitor, TM: thrombomodulin, APC: activated protein C.

Figure 2. Cell-Based Model of Coagulation.

This model depicts the involvement of cells in the initiation, propagation, and amplification of coagulation. Coagulation factors are in roman numerals. Activated forms are indicated by the letter 'a'. TF: tissue factor, vWF: von Willebrand Factor, Fg: fibrinogen, Fb: fibrin.

1.1 Coagulation

In the past, to better understand blood coagulation, the waterfall cascade was used to explain the activation of coagulation factors (10). In this model there are two pathways in which coagulation can be activated. Firstly, the extrinsic pathway is initiated by the exposure of tissue factor (TF) on subendothelial cells leading to the activation of factor VII to VIIa (VIIa) (1,2,11,12). VIIa then forms the extrinsic tenase complex with TF and Ca^{2+}, which will activate factor X to Xa (1,11). Xa then forms the prothrombinase complex (in the presence of Ca^{2+} on phospholipid surfaces) with its cofactor, factor Va (Va), and prothrombin (II) to produce thrombin (IIa) (1,10,11,13,14) (Fig. 1).

The extrinsic pathway converges with the intrinsic pathway of coagulation at the point of Xa activation (1). The intrinsic pathway (also known as contact pathway) is triggered by factor XII activation to XIIa, upon contact with negatively charged surfaces, such as collagen, extracellular DNA, and RNA (2,10). This causes the activation of factors XI and IX to XIa and IXa, and formation of kallikrein. This leads to the formation of the intrinsic tenase complex (Ca^{2+}, VIIIa, IXa) on phospholipid surface, to form more Xa followed by the production of more IIa, through the prothrombinase complex (1,2). IIa will then amplify its own production through feedback activation of factors XI, IX, VIII, and V (1,2,11,14). Also, most importantly, IIa will cleave fibrinopeptides A and B (FPA and FPB) from the N-terminus of Aα and Bβ chains of fibrinogen to form fibrin monomers and eventually lead to formation of a clot (Fig. 1) (15).

This model accurately depicts the overall process of the proteolytic activation of coagulation factors and has been deemed useful in describing coagulation *in vitro*. However more recently it has been observed that coagulation involves surrounding cells such as platelets and endothelial cells (12). This cell-based model occurs in three phases: initiation, amplification,

4

and propagation (Fig. 2). Initiation occurs following blood vessel injury in which TF on subendothelial cells interact and activate factor VII to VIIa (12,16). VIIa will activate factor X (as previously mentioned in the coagulation cascade) and also factor IX leading to a small production of IIa (17). While this is occurring, the disruption in vessel wall causes externalization of platelet adhesion molecules (such as P-selectin) and release of von Willebrand Factor (vWF) from Weibel Palade bodies (WPD) in endothelial cells (18). vWF from endothelial cells and the circulation will also accumulate to exposed collagen in the subendothelium (12,19). This initiates local platelet adhesion and activation through binding of vWF and collagen to platelet glycoproteins, GPIbα and GPVI, respectively (19,20). Aggregating platelets are in close proximity to TF bearing subendothelial cells, and thus the IIa that was previously produced is now able to activate platelets by binding protease-activated receptors (PAR) (21). Platelet activation results in the release of granule contents such as AT, protein S, factor V and fibrinogen (19,22). Along with its conversion to fibrin, fibrinogen binds to GPIIb/IIIa on neighbouring platelets to cross-link them together (16).

Concurrent, with platelet activation and accumulation, is the amplification phase of coagulation. The expression of phosphotidylserine, on phospholipids from platelet activation, provides a procoagulant surface for IIa mediated reactions. These include the release of factor VIII from vWF and its subsequent activation to VIIIa. As well, IIa activates factor V (to Va). Activated factor VIII (VIIIa) and V (Va), are cofactors to IXa and Xa respectively, and thus lead to the generation of more IIa (10,23,24). IIa can also activate factor XI, from the intrinsic pathway, that is localized to platelets via GPIbα receptor (24,25). It is also suggested that factor XII can localize to the site of thrombus formation, on platelets, by interacting with the same

receptor, leading to possible collagen mediated activation of the intrinsic pathway (Fig. 2) (23,26).

In the propagation phase, the IXa/VIIIa and Xa/Va complexes are assembled on activated platelet surfaces to generate Xa and IIa, respectively (16,24). The activated factor XI (XIa) will also produce more IXa. This results in a large production of IIa, followed by the cleavage of fibrinogen into fibrin to form a network on the platelet surface (23,27). In addition, platelets localize factor XIII on integrin αIIbβ3 for IIa activation, which leads to the cross-linking and stabilization of the fibrin clot (28,29).

1.2 Antithrombin

In order to localize coagulation to the site of injury and prevent unwanted downstream clotting, there are several proteins involved in anticoagulation. The most potent anticoagulant is a liver synthesized, plasma glycoprotein (MW ~ 58,000 Da), antithrombin (AT) (4,30). It is responsible for the inhibition of coagulation factors, IXa, XIa, XIIa, VIIa, and most importantly IIa and Xa (Fig. 1) (1). AT has two major circulating forms, 90% as α-AT and 10% as β-AT, based on differences in glycosylation (4,30). α-AT possesses N-linked glycans on asparagine residues 96, 135, 155, and 192 whereas β-AT lacks a glycan on asparagine 135 (31,32).

AT is a serine protease inhibitor (serpin) consisting of a reactive center loop (RCL), three β-sheets and nine α-helices in its structure (30). AT inhibition occurs through a typical serpin mechanism by which the RCL binds to the active site of the serine protease (4). The serine protease cleaves P1-P1' residues on AT, causing the insertion of the RCL into a β-sheet and ultimately forming an inactive acyl-enzyme complex (4,30).

1.3 Heparin

Heparin (H) is a sulfated glycosaminoglycan (MW = 3000 to 30,000 Da) produced by mast cells (1,33,34). The rate of AT inhibition of Xa and IIa is relatively slow but when H binds to AT, the rate of inhibition of Xa and IIa can be increased up to 580 and 4,300-fold respectively (4,30,35). H binds AT around the D helix and it is noted that β-AT has a higher affinity for H compared to α-AT (30-32).

H mediates AT inhibition of Xa via a conformational change mechanism (Fig. 3). This involves binding of the pentasaccharide sequence of H to AT which results in the expulsion of the RCL, allowing for better access by Xa (4). In contrast, IIa inhibition occurs through the template mechanism (Fig. 3). H acts as a bridge to bring AT and IIa into close proximity (4). Along with the pentasaccharide sequence, this mechanism requires longer chain lengths of H, at least 18 saccharides, to increase IIa binding at non-specific sites (4,33) (Fig. 3).

The ability of H to enhance AT inhibition of coagulation factors has been deemed useful in treating thrombotic related diseases (1,4,34). However, due to its heterogeneous structure, only about one-third of administered unfractionated heparin (UFH) contains the pentasaccharide sequence, required for AT binding (34). As well, UFH use has been associated with H induced thrombocytopenia (HIT), unwanted interaction with platelets/endothelial cells/proteins, unpredictable dose responses, and a short half-life (34).

These limitations have led to the synthesis of low molecular weight heparin (LMWH), which consists of fragments of H produced by depolymerization with chemicals or enzymes (34). LMWH is approximately one third the size of UFH (mean MW = 5000 Da) (36). Due to its decreased size, LMWH interacts less with proteins and other cells, thus increasing its half-life (34). This may also explain the more predictable dose dependent response observed, in

comparison to UFH (34). LMWH and UFH have similar Xa inhibition abilities, however, the

ability of LMWH to inhibit IIa, is decreased as only 25-50% of LMWH have chains longer than

18 saccharides (36).

A Conformational Change Mechanism

Unfractionated Heparin

Factor Xa

+

Pentasaccharide Sequence

Antithrombin

Thrombin

B Template Mediated Mechanism
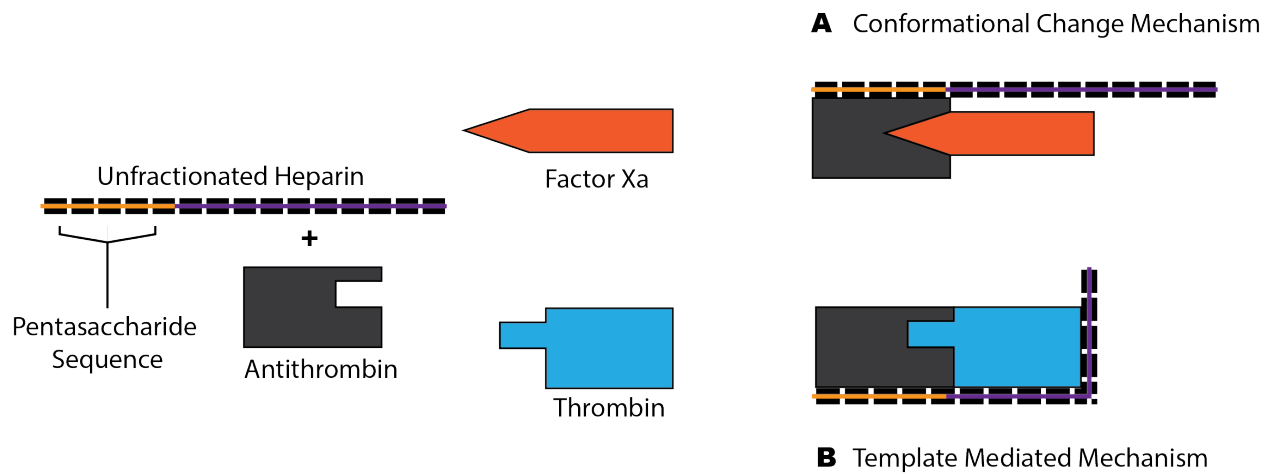
Figure 3. Conformational Change and Template Mediated Mechanism of Antithrombin.
(A) Facilitation of antithrombin inhibition of Factor Xa by heparin, through a conformational change mechanism. (B) Antithrombin inhibition of thrombin catalyzed by heparin through a template mediated mechanism.

1.4 Antithrombin-Heparin Covalent Complex (ATH)

The limitations of both UFH and LMWH led to the synthesis of an improved anticoagulant. Chan et al., synthesized a novel anticoagulant, antithrombin-heparin covalent complex (ATH) that has a more effective anticoagulant ability against IIa, Xa and other coagulation factors, when compared to mixtures of AT and UFH/HASH (high affinity standard heparin) (37). ATH has increased intravenous half-life and decreased interactions with plasma proteins, both of which are limitations of UFH (37,38).

1.4.1 Preparation of ATH

ATH (MW = 69,000-100,000 Da) is prepared by heating AT and excess UFH in buffer for 14 days at 40 °C (37,38,39,40). During the incubation period, non-covalent binding of AT to the pentasaccharide sequence of UFH allows for a Schiff-Base (imine) formation between the aldehyde group on UFH and primary amino groups on AT. This metastable intermediate then undergoes an Amadori rearrangement to yield a stable keto-amine (37,39,40). Further incubation with NaBH$_3$CN in buffer is conducted to reduce any Schiff base that was not stabilized by the Amadori rearrangement (37). ATH is then isolated with hydrophobic chromatography that removes unbound UFH. This is followed by DEAE Sepharose chromatography, to remove unbound AT (39). This method of synthesis produces a percent yield of approximately 50% ATH with 55% containing α-AT and 45% β-AT (as β-AT has higher affinity for UFH) (41).

1.4.2 ATH and its Anticoagulant Properties

As mentioned, the inhibition of Xa and IIa by ATH is more effective over mixtures of AT and UFH/HASH when using commercial assay kits (37). As well, clot bound IIa is generally protected from AT + H, however, ATH is able to overcome this (5,40,42-44). H binds to fibrin and forms a fibrin-H-IIa ternary complex that resists approach by noncovalent AT + H

complexes (40,45). It was found that the H chain of ATH is able to bind in this manner and allow for covalently bound AT to inhibit IIa bound to fibrin (40,44). In addition, the H chain in ATH, bound to fibrin clots, is able to facilitate inhibition of fluid phase IIa by exogenous AT (40). This describes the catalytic mechanism of ATH, in which its H chain can bind circulating AT and thus inhibit more IIa (Fig. 4) (46).

In addition to enhanced inhibition of clot bound IIa, *in vitro* studies have shown ATH is able to inhibit Xa in the prothrombinase complex, which is otherwise protected from plasma AT (43,47-49). In the same study by Stevic et al., inhibition of Xa in prothombinase also led to a decrease in IIa generation (47).

In vivo studies further support ATH's efficacy as an anticoagulant (6,44,50). In a rabbit venous thrombosis model, ATH was able to decrease clot mass and fibrin accretion, while administration of AT, standard H (SH), or AT + UFH resulted in an increase in both measures (6). Similarly, in a rabbit arterial thrombosis model, ATH was able to prevent clot formation following vessel injury, while SH, at similar doses, resulted in detectable clots (44). In a rabbit bleeding ear model, ATH treatment displayed a decreased risk of bleeding when compared to SH (44). Lastly, in a pig cardiopulmonary bypass model, ATH was able to decrease the number of micro-emboli when compared to UFH (50).
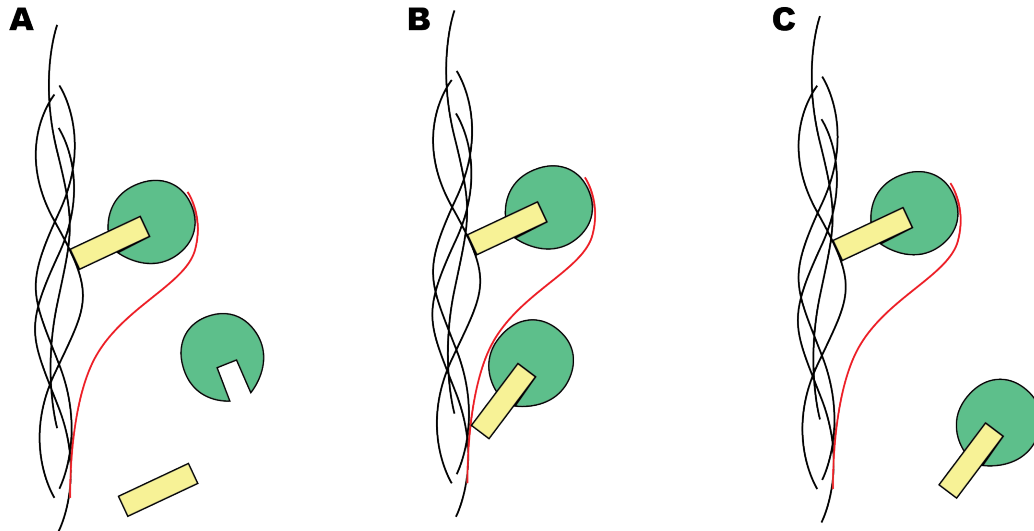
Figure 4. Direct and Catalytic Inhibition Mechanism of Action of ATH.

(A) Antithrombin-heparin covalent complex (ATH) inhibits fibrin (back) bound thrombin (yellow) via direct inhibition. (B) The heparin chain (red) in ATH can also simultaneously facilitate inhibition of free thrombin by exogenous antithrombin (green), through the catalytic mechanism. (C) Thrombin forms an inactive complex with exogenous antithrombin.

1.5 Fibrinolysis

Coagulation and IIa generation are highly regulated processes. As mentioned earlier, these processes interact with another pathway, fibrinolysis, the process of fibrin degradation and clot breakdown (51). Fibrinolysis begins with the interaction of several coagulation factors with endothelial cells to stimulate the increased release of tissue-type plasminogen activator (tPA)(52). tPA functions as a single or two chain serine protease with two Kringle regions (51). It cleaves plasminogen (Pg), a proenzyme, between Arg 561-Val 562 to produce activated plasmin (Pn) (15,51,53). Another Pg activation pathway is through cleavage by urokinase-type plasminogen activator (uPA) (15). However, this process is predominantly responsible for degradation of extracellular matrix and not fibrinolysis (Fig. 1) (15,54). Efficient tPA activation of Pg to Pn requires fibrin which can enhance the reaction up to three folds, yet fibrin is not required for uPA (15,53). tPA binds to fibrin through its second Kringle domain or its finger like domain, while Pg binds to carboxy-terminal lysine residues on α, β, and γ chains, forming a ternary complex for Pn generation (15,51).

Pg circulates in plasma as Glu- or Lys-Pg (MW = 90, 000 and 83,000 Da) at a concentration of 1.5-2 μM (53,54). Pg is synthesized in the liver as a single chain glycoprotein containing five Kringle domains (51,53,54). Once formed, Pn cleaves fibrin into X-oligomers, which are further degraded to E and D-dimers containing two covalently bound D-domains (15). During fibrin degradation, more carboxy-terminal lysine residues are exposed which facilitate more Pg conversion to Pn by tPA (Fig. 5) (51).

1.5.1 Regulation of Fibrinolysis

There are several regulators of fibrinolysis that inhibit Pn generation or Pn activity. Plasminogen activator inhibitor 1 (PAI-1) is a serpin responsible for the inhibition of tPA and uPA, in the presence of its cofactor, vitronectin (15,53). Also, activated thrombin activatable fibrinolysis inhibitor (TAFIa) removes C-terminal lysine residues from fibrin, which prevents additional binding of Pg and tPA, thus down regulating Pn generation.

As Pn is a serine protease, it is inhibited by several serpins, with its main inhibitor being α_2-antiplasmin (α_2-AP). α_2-AP is a rapid inhibitor that forms inactive equimolar complexes with free Pn (54). It is found at concentrations of 1 μM in plasma (54). In addition, Pn can be inhibited by α_2-macroglobulin (α_2-M) (a general protease inhibitor) and AT (54-56).
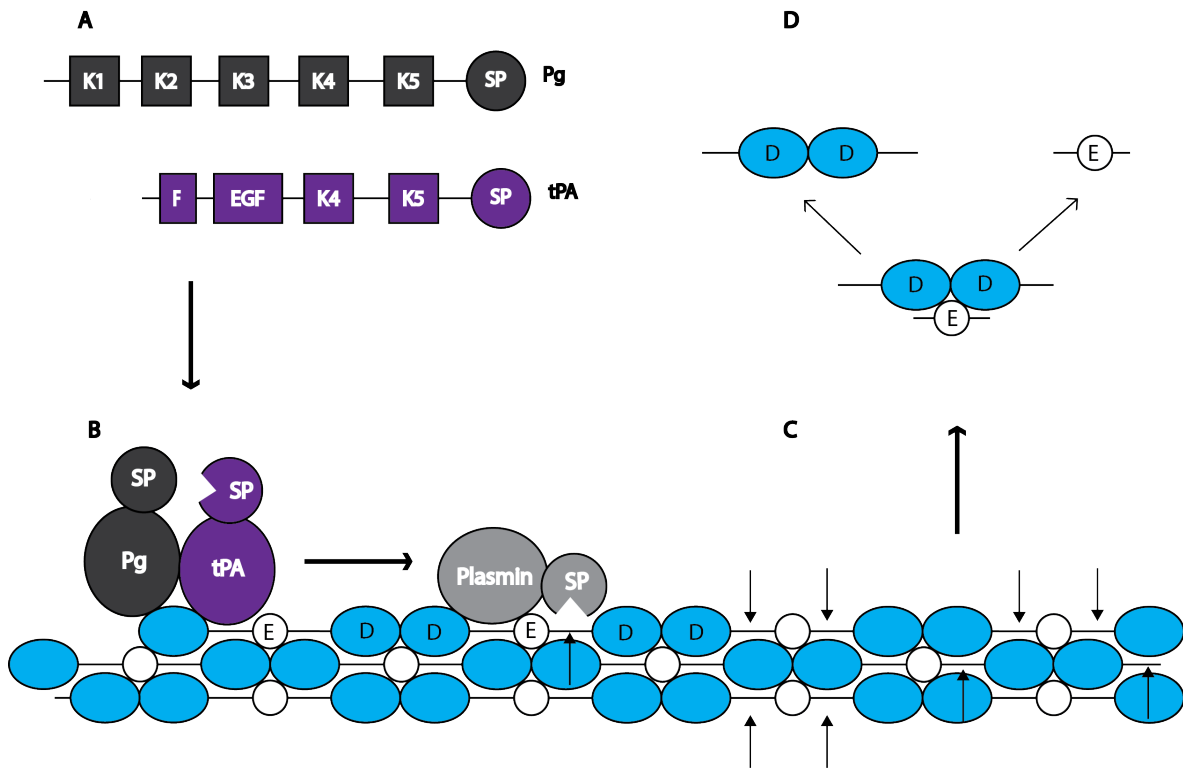
Figure 5. Structures of Plasminogen & tPA and Mechanism of Fibrin Degradation by Plasmin.

(A) Structures of plasminogen (Pg) and tissue-type plasminogen activator (tPA). (B) Activation of plasminogen to plasmin by tPA via formation of ternary complex. (C) Cleavage of fibrin at D and E regions to generate carboxy-terminal lysine residues. (D) Fibrin degradation products as D-dimer and E-fragment. EGF: EGF-like, F: Finger-like, K: Kringle-like, and SP: serine protease modules.

1.6 Heparin and Fibrinolysis

H has been found to have variable effects on fibrinolysis. Depending on the study and experimental conditions, H can enhance (57-68), inhibit (69), or have no effect on fibrinolysis (60,70).

1.6.1 Heparin and Plasmin Inhibition

One known interaction of H and fibrinolysis is through H mediated AT inhibition of Pn (9,71,72). H itself has no effect on Pn activity but it was suggested that H enhances AT inhibition of Pn through a conformational change mechanism (9,72). *In vitro* studies, in purified systems, indicate H can increase Pn inhibition by AT up to 50-100 fold (9,55,71,73). Further studies show AT forms stable 1:1 stoichiometric complexes with Pn (9,55,71-73).

In vitro studies in plasma indicate a H dose dependent response in the formation of Pn-AT-H complexes (55). In α_2-AP and α_2-M depleted plasma the amount of Pn bound to AT was higher than that of normal plasma, in the presence and absence of H (55). This indicates that although H enhances AT inhibition of Pn it may contribute minimally to anti-plasmin activity, as α_2-AP and α_2-M have higher affinities for Pn (55,71,74). More recent studies by Chander et al., comparing the effects of UFH + AT and ATH on Pn inhibition rates, found they were 2-3 orders of magnitude lower than the inhibition of other coagulation factors, which is consistent with previous studies (9,55,56,71,74). Similar results were found with *in vivo* studies of patients receiving thrombolytic therapy as it was concluded only 3-11% of Pn formed was inhibited by AT bound to H (56).

1.6.2 Heparin and tPA Mediated Plasminogen Activation

It has been observed in the past, *in vitro and in vivo,* that UFH and high molecular weight H (HMWH) can decrease euglobulin lysis time (ELT) signifying enhancement of fibrinolysis (67). In particular, some studies have shown that H can enhance tPA mediated Pg conversion to Pn (57,58,60,62-64,66,68). *In vitro* studies, in buffer systems, found that UFH can accelerate Pn generation up to 5-folds in a dose dependent relationship (66). The stimulation of tPA conversion of Pg to Pn by H is reduced in the presence of fibrin or fibrin substitutes, which have a higher affinity for tPA (59,60,62,64,66). As well, there is no additive stimulating effect on tPA when H and fibrin are both present which suggest they compete for the same binding site on tPA (59,60,62,64,66).

On the other hand, LMWH does not seem to stimulate Pn generation or enhance fibrinolysis (66,67). This could possibly be due to its short chain length, which can only bind tPA, whereas longer oligosaccharides can bind both tPA and Pg, bringing them in closer proximity (58). Other evidence proposes that H interacts with tPA's fingerlike domain or another site, causing a conformational change that favours Pg binding (57,59,68).

More *in vitro* studies have shown that H could have no effect (in plasma) (69,70,75) or even inhibit Pn generation (in buffer) (69). This could partly be due to the variation in assay systems, ionic strength, and the presence of divalent cations or chloride ions (69,70). It was found that increasing ionic strength in the presence of H causes inhibition of Pg activation, followed by enhancement of activation at higher ionic strengths (69). As well, divalent cations, such as Ca^{2+} and Mg^{2+} can cause up to a 60-fold increase in H accelerated Pg conversion to Pn (69). Lastly, the presence of chloride ions can induce a less accessible conformational change in Pg and will inhibit Pn generation in the presence of H (69).

1.7 ATH and Fibrinolysis

Due to the discrepancies of results in past studies, more recent studies, *in vitro*, were aimed at revisiting H's effect on Pn activity and Pn generation under more ideal conditions of 37 °C, physiological pH and ionic strength (9). Chander et al., used second order rate constant assays to observe the rate of Pn inhibition by mixtures of AT + UFH compared to ATH, in order to further understand the mechanism behind the interaction of the H moiety in ATH (9). It was confirmed that free Pn can be inhibited by AT + UFH (k_2 = 5.74 × 10^6 $M^{-1}min^{-1}$) and this inhibition is decreased in the presence of fibrin (k_2 = 1.45 × 10^6 $M^{-1}min^{-1}$). This indicates Pn is protected from inhibitors when bound to fibrin (9). Likewise, Pn inhibition by ATH was observed in the absence of fibrin (6.39 × 10^6 $M^{-1}min^{-1}$). Although ATH inhibition of Pn decreased in the presence of fibrin (3.07 × 10^6 $M^{-1}min^{-1}$), the k_2 value was higher than that of AT + UFH, suggesting enhanced inhibition of Pn by ATH, even in the presence of fibrin (9).

Chander et al., also studied the rate of Pn generation on fibrin clots, in the absence or presence of AT + UFH, ATH, or UFH (9). The rate of Pn generation was decreased in the presence of AT + UFH and ATH but not with UFH. It was noted that ATH reduction in Pn generation was greater than that of AT + UFH. In order to investigate whether this reduction in Pn generation was due to the anticoagulants' interaction with tPA or inhibition of Pn itself, tPA chromogenic activity was tested in the presence of AT+ UFH, UFH, and ATH. Results showed there were no differences in tPA activity when each anticoagulant was present indicating an inhibition of Pn and not alteration of tPA activity during Pn generation (9).

1.8 Overall Objective

The main objective of this study is to observe and compare the effects of UFH, LMWH and ATH on Pn generation in plasma, to further understand the effects of these anticoagulants on fibrinolysis in a more physiological system.

1.9 Hypothesis and Rationale

There has been much debate on H's effect on fibrinolysis, whether it affects tPA mediated Pn generation or Pn activity. H on its own has no effect on Pn activity, but when coupled with AT, it can increase AT's ability to inhibit free Pn (9,66,71,72,72). I*n vitro* studies show H facilitated Pn inhibition occurs in a dose dependent manner, possibly through a conformational mechanism (9,55,72). Yet other studies suggest H can enhance tPA conversion of Pg to Pn, as it interacts with fibrin binding sites on tPA (57-60,62-64,66,68).

More recent studies in buffer systems, by Chander et al., confirmed that mixtures of AT + UFH do, in fact, inhibit Pn activity and can also inhibit Pn generation. To further identify the mechanism, tPA chromogenic activity was tested in the presence of UFH and AT + UFH and it was found that there was no change in tPA activity. Consequently, the decrease in observed Pn generation was due to inhibition of plasmin itself (9). Based on these results, it is hypothesized that in this study UFH and LMWH will facilitate AT (present in the plasma) inhibition of Pn generated leading to a decrease in quantified Pn over time (hypothesis 1).

In addition, Chander et al., observed that ATH could inhibit free Pn in the presence and absence of fibrin(ogen) more effectively than AT+ UFH. Also, ATH was able to reduce Pn generation more than AT + UFH. This effect of ATH on Pn is consistent with past studies regarding H facilitated inhibition of Pn (55,56,66,71-73). Thus, it can be thought that in this plasma system, ATH will similarly inhibit Pn generation but to a greater extent than UFH or

LMWH due to its increased ability to inhibit serine proteases compared to mixtures of AT + UFH (hypothesis 2).

These past studies have also suggested that AT inhibition of Pn is relatively slow (even in the presence of H) and may have a minimal effect in the presence of its natural inhibitors: α_2-AP and α_2-M (9,55,56,71,74). As a result, in plasma, α_2-AP and α_2-M, will compete with UFH and LMWH bound AT and ATH for inhibition of the Pn generated. The presence of UFH and LMWH will lead to a decrease in α_2-AP and α_2-M-bound Pn (PAP and PAM complexes respectively) as UFH and LMWH accelerates AT inhibition of Pn (hypothesis 3). Lastly, since ATH has been proven to be a stronger inhibitor of Pn than mixtures of AT + UFH, the presence of ATH will decrease PAP and PAM complexes to a greater extent than UFH and LMWH (hypothesis 4) (9).

1.10 Specific Aims

1) To develop an assay system that will allow for the quantification and observation of Pn generation over time.

2) To take the assay system from aim 1 and add UFH, LMWH, and ATH at various doses to compare their effects on Pn generation.

3) To quantify Pn bound to α_2-AP (PAP) and α_2-M (PAM) to further understand observations produced in aims 1+ 2.

4) To quantify Pg consumption during Pn generation under the same conditions as aim 2

2 Experimental Procedures

2.1 Materials

2.1.1 Reagents

All reagents used were of analytical grade. Tris (hydroxymethyl) aminomethane and sodium chloride (NaCl) were purchased from Bioshop (Burlington, ON). Polyethylene glycol 8000 (PEG 8000) and ethylenediamine tetraacetic acid (EDTA) were purchased from BDH Inc. (Toronto, ON). HEPES, Bovine serum albumin (BSA), and Tween 80 were purchased from Sigma Aldrich (St. Louis, MO, USA). Sodium phosphate monobasic monohydrate ($NaH_2PO_4 \bullet H_2O$) and sodium phosphate dibasic anhydrous (Na_2HPO_4) were purchased from EM Millipore (Darmstadt, Germany).

2.1.2 Anticoagulants

UFH (lot #: 083K1142) was purchased from Sigma (Mississauga, ON). LMWH (Tinzaparin), was purchased from Leo Pharma Inc. (Thornhill, ON). ATH (lot #: 031120) was produced by methods previously described (21,23,24).

2.1.3 Proteins

Normal Human Pooled Plasma (NPP) (lot #: NPP-0031) and Plasminogen Deficient Plasma (PgdP) (lyophillized) (lot #: LP21-005) were purchased from Affinity Biologicals (Ancaster, ON). Human Plasmin (Pn) and Glu-Plasminogen (Glu-Pg) were purchased from Enzyme Research Laboratories (South Bend, USA). Human PAI-1 stable mutant and Human tPA (> 95% two-chain) were purchased from Molecular Innovations Inc. (Novi, MI, USA). Cyanogen Bromide Fibrinogen Digest (Fib) (Pg and Pg activator depleted) was purchased from Sekisui Diagnostics (Stamford, CT, USA). Trypsin Inhibitor from Glycine max (soybean) (SBTI) and α_2-Macroglobulin (α_2-M) was purchased from Sigma Aldrich (St. Louis, MO, USA).

2.1.4 Storage of Proteins

All stock proteins were stored in eppendorf tubes at -80°C. Human Pn was diluted to 6 µM in PBS (0.016 M Na_2HPO_4, 0.004 M $NaH_2PO_4 \bullet H_2O$, 0.15 M NaCl, pH 7.2-7.4). Human PAI-1 was diluted to 4.941 µM in PES (0.05 M $NaH_2PO_4 \bullet H_2O$, 1 mM EDTA, 0.1 M NaCl, pH 6.6). Human tPA was diluted to 595 nM in HBS + BSA (0.4 M Hepes, 0.1 M NaCl, 1% BSA, pH 7.4). Fib was re-suspended in milli-Q water to a concentration of 2.5 mg/ml. PgdP (lyophilized) was reconstituted with 1 mL of milli-Q water. SBTI was reconstituted with reverse osmosis purified water to 248.76 µM. α_2-M was reconstituted and stored at 5 mg/ml in HBS (0.02 M Hepes, 0.15 M NaCl, pH 7.4).

2.1.5 ELISA Kits

The Technozym Glu-Plasminogen ELISA kit and PAP Complex ELISA kit were purchased from Technoclone GmbH (Vienna, Austria).

2.1.6 Enzyme Substrates

Chromogenic substrate for Plasmin (S2251) was purchased from Molecular Innovations Inc. (Novi, MI, USA) or Chromogenix (Bedford, MA, USA).

2.2 Methods

A SpectraMax Plus 384 Spectrophotometer (Molecular Devices, CA, USA) combined with SOFTpro Max Version 5.4.1 was used to measure absorbance of cleaved chromogenic substrate at a wavelength of 405nm wavelength or turbidity change at 450 nm.

2.3 Plasmin Activity Standard Curve in Plasma

A Pn activity standard curve was produced in order to convert absorbance (OD) measured to Pn concentration (nM) by plotting known concentrations of purified human Pn against absorbance. In brief, Pn was diluted in TSP to concentrations of 0, 10, 20, 40, 80, 160,

300, and 400 nM. Each Pn concentration was incubated with S2251 (0.5 mM) at 37°C for 20 mins. The reaction was then stopped with 50% acetic acid and OD was measured at 405 nm.

2.4 Optimization of Plasmin Generation Assay in Plasma

2.4.1 Testing for PAI-1, tPA, Fib activity against S2251

PAI-1 (44.65 nM), Fib (150 µg/ml), or tPA (89.25 nM) was incubated with excess S2251 (0.5 mM) in TSP, in a 96-well microtiter plate. Change in absorbance over time (mOD/min) was measured every 10 seconds (s) for 20 mins at 405 nm.

2.4.2 Testing PAI-1 Inhibition of tPA

PAI-1 (44.65 nM) was added to tPA (0.8925 nM) in TSP in microtiter wells and allowed to incubate for 0, 30, 60, 90, 120, and 180 s. Then, 172 µl of the PAI-1/tPA solution was added to 10 µl of normal pooled plasma (NPP). Then, 18 µl of S2251 was added and any Pn produced, as a result of residual tPA activity, was quantified with S2251 as previously described.

2.5 Plasmin Generation Assay in Plasma

The protocol for Pn generation was adopted from Parmar et al., with some modifications (82). tPA and Fib were diluted in TSP. At 37 °C, an equal volume (90 µl) of NPP was added to initiate Pn generation. According to previous studies, Fib will provide a surface for the acceleration of tPA activation of Pg to Pn (76-80). After addition of NPP, tPA and Fib concentrations were 8.925 nM and 300 µg/ml respectively. Subsamples (20 µl) of the reaction were taken at specific time points (0, 0.5, 1, 2, 5, 10, 20 and 60 mins) and further Pn generation was inhibited by the addition of 162 µl of plasminogen activator inhibitor-1 (PAI-1) at a ratio of 1:50 (tPA:PAI-1 concentration) in a 96-well flat microtiter plate. 18 µl of S2251 (0.5 mM) was added to each well and allowed to incubate for 20 mins. At 20 mins, 50 µl of 50% acetic acid was added to stop further Pn cleavage of S2251. Absorbance emitted by Pn cleavage of p-

nitroaniline on S2251, at each time point, was measured at 405 nm (at 37 °C) and Pn was quantified using the Pn standard curve.

To study the effects of anticoagulants on Pn generation, several doses (0.35, 0.7, 1.4, and 2.1 U anti-Xa activity/ml) of UFH, LMWH, and ATH were added into NPP before initiating the Pn generation reaction. ATH was also added to NPP at lower doses (0.001, 0.01, 0.02, 0.05, and 0.1 U/ml). The Pn generation assay was conducted as described above.

2.5.1 Plasmin Generation using Various Concentrations of tPA and Fib

Pn generation was conducted, as described above, with varying combinations of tPA (4.464 and 8.928 nM) and Fib (0, 150, 300, 600 µg/ml) concentrations.

2.5.2 Plasmin Generation with Pg Deficient Plasma

To confirm that the chromogenic activity during Pn generation experiments was due to the conversion of Pg to Pn, Pg deficient plasma (PgdP) was used to replace NPP in several Pn generation experiments (without anticoagulants) and compared to experiments conducted with NPP.

2.6 Quantification of PAM Complexes

2.6.1 Testing for Soybean Trypsin Inhibitor Effectiveness on Plasmin

The following experiment was conducted to ensure SBTI inhibited free Pn effectively. 50 µl of Pn-α_2-M (PAM) complexes were synthesized by mixing excess α_2-M (720 nM) with 500 nM of Pn in TSP. Separate solutions of Pn (500 nM) and 720 nM of α_2-M in TSP were prepared as controls. The solutions were incubated at room temperature for 6 hours and then stored at -80 °C for later use.

At 37 °C, the three solutions above were thawed and diluted to 1/10 in TSP. 20 µl of diluted PAM, Pn, or α_2-M was added to separate wells in a 96-well microtiter plate followed by

the addition of 162 μl of PAI-1 (55.1 nM) ± SBTI (5 μM) to inhibit any remaining free Pn.

These reactions were incubated for 2 mins, followed by the addition of 18 μl of S2251 (0.5 mM).

The substrate was allowed to react with PAM, Pn or α_2-M for 20 mins. The reaction was stopped

with 50 μl of 50% acetic acid. Remaining Pn amidolytic activity reflected by absorbance was

measured at 405 nm and 37 °C.

2.6.2 Assay to Quantify PAM Complexes

Pn generation was conducted similarly to Section 2.5, with the following changes.

Subsamples were taken at time points of 0, 10, 20, and 60 mins and added to 162 μl of PAI-1

(55.1 nM) ± SBTI (5 μM). This was then followed by the addition of 18 μl of S2251 (0.5 mM)

for quantification of Pn activity. In the presence of SBTI, all free Pn will be inhibited, and

remaining Pn activity will be reflective of PAM complexes. These experiments were conducted

in the presence and absence of 0.35 and 0.7 U/ml of UFH or ATH. At the same time points, 20

μl subsamples were also added to 162 μl of PAI-1 (55.1 nM) in eppendorf tubes, followed by the

addition of 18 μl of TSP. These subsamples were stored at -80 °C for later use in PAP complex

and Pg quantification by ELISA.

2.7 Quantification of PAP Complexes Produced During Plasmin Generation with Technozym PAP ELISA Kit

Pre-coated microwells (monoclonal antibody against neoantigen in PAP complex), wash

buffer (PBS, pH 7.3), dilution buffer (PBS, pH 7.3), PAP high/low calibrators, standards, POX

conjugate, substrate (TMB), and stop solution (sulphuric acid) were provided by the kit. The

protocol according to the package insert from Technozym PAP Complex ELISA kit

(Technoclone GmbH) was performed. Subsamples taken from previous Pn generation

experiments (Section 2.6.2) were diluted 1:1000 in dilution buffer. 100 μl of the subsamples,

calibrators, and standards were added in duplicate to pre-coated wells. Samples were incubated overnight at 4 °C followed by four washes with 200 µl of wash buffer. A volume of 100 µl of POX conjugate was added to the wells and allowed to incubate for 2 hours at 37 °C. Wells were washed again as described and 100 µl of substrate was added. After 20 mins 100 µl of stop solution was added to wells and the absorbance was measured at 450 nm and 620 nm. The absorbance at 620 nm was subtracted from that measured at 450 nm to obtain final absorbance values. Absorbances were converted to PAP concentrations by comparison with the standards.

2.7.1 Testing the Specificity of the Technozym PAP Complex ELISA

Several controls were tested using the ELISA kit, prior to testing Pn generation subsamples. NPP, 1 µM Pn, 2 µM PAM complexes, 0.7 and 2.1 U/ml of UFH or ATH in NPP were diluted 1:1000 in dilution buffer and the PAP ELISA was conducted as previously described (Section 2.7). The specific concentrations of the above reagents were selected to resemble corresponding amounts that might be found in Pn generation subsamples.

2.8 Quantification of Plasminogen Consumption During Plasmin Generation with Technozym Plasminogen ELISA Kit

Pre-coated microwells (monoclonal anti-Pg antibody blocked with 1% BSA), wash buffer, incubation buffer, glu-Pg standard, POX antibody (polyclonal anti-Pg antibody), substrate (TMB), and Stop solution (sulphuric acid) were provided by the kit. The protocol according to the package insert from Technozym Pg ELISA Kit was performed. Subsamples taken from previous Pn generation experiments (Section 2.6.2) were diluted 1:1000 in incubation buffer. A volume of 100 µl of each subsample and standards were added in duplicate to pre-coated microwells. Samples were covered and allowed to incubate overnight at 4 °C. The plate was washed five times with 250 µl of wash buffer followed by the addition of 100 µl of POX

antibody. The antibody was incubated in the wells for 1 hour at 37 °C followed by washing the

plate five times, as previously described. A volume of 100 μl of substrate was added to samples.

After 15 mins at room temperature, 100 μl of stop solution was added and the absorbance was

measured at 450 nm and 620 nm. The absorbance at 620 nm was subtracted from that measured

at 450 nm to obtain final absorbance values. Absorbances were converted to Pg concentrations

by comparison with the standards.

2.8.1 Testing the Specificity of the Technozym Plasminogen ELISA Kit

Several controls were tested in the ELISA kit prior to testing Pn generation subsamples.

NPP, 0.5 μg/ml Pn, 0-5.5 μg/ml Glu-Pg, 0.7 and 2.1 U/ml UFH/ATH in NPP, PgdP, 0.5 μg/ml

Pn in PgdP, and 0.5 μg/ml Pg in PgdP were diluted 1:1000 in incubation buffer and the Pg

ELISA was conducted as previously described (Section 2.8). Concentrations of the above

reagents were selected to resemble what may be found in Pn generation subsamples from Section

2.6.2.

2.9 Specific Activity of Plasmin against S2251 in Plasma on a Fibrin Clot

To accurately quantify Pn concentrations during Pn generation on fibrin clots, 90 μl of

S2251 in NPP was added to 5 μl of various concentrations of Pn and 5 μl of Ancrod in TBS-T80

(50 mM Tris-Cl, 0.1 M NaCl, 0.01% Tween 80, pH 7.4). The final concentrations of S2251, Pn,

and Ancrod were 0.4 mM, 0-650 nM, and 0.6 U/ml, respectively. Absorbance was measured

every 10 s for 2 hours at 405 nm (indicating S2251 cleavage by Pn) and 450 nm (reflecting

turbidity change and clot formation). The change in absorbance over time of the corrected

absorbance values (Acorr) (mOD/min) was plotted against corresponding Pn concentrations (0-

700 nM) and fit to a linear trendline (refer to Section 2.15.3 for calculation of Acorr). The slope

of this trendline was termed the specific activity (SA) of Pn against S2251. SA was used to convert subsequent measured absorbances over time, into Pn concentrations.

2.10 Optimization of Plasmin Generation Assay on Fibrin Clot

To further observe the effect of UFH and ATH on Pn generation, a Pn generation assay on a fibrin clot was adapted from Chander et al., with some changes (9).

2.10.1 Optimization of Ancrod Concentration

To optimize for Ancrod concentration, 90 μl of NPP in TBS-T80 was added to 10 μl of increasing concentrations of Ancrod (0-20 U/ml) to initiate fibrin clot formation (final NPP was diluted 1/3). Turbidity was measured at 37 °C for 2 hours every 10 s at 450 nm. Ancrod concentration that allowed for full clot formation that remained stable for at least 3 mins was deemed appropriate.

2.10.2 Optimization of tPA Concentration

The concentration of tPA that resulted in a clot-lysis time of approximately 30 mins was established as an acceptable time frame. This would provide sufficient time for Pn generation rates to be assessed while the clot was stable. NPP diluted in TBS-T80 was added to 5 μl of Ancrod and 5 μl of various concentrations of tPA. The dilution of NPP was 1/3 and final concentrations of Ancrod and tPA were 0.6 U/ml and 0-90 nM, respectively.

2.11 Plasmin Generation on a Fibrin Clot

To measure Pn generation rates, 90 μl of NPP in TBS-80 and S2251 ± UFH/ATH (pre-warmed to 37 °C) was added to wells containing 5 μl of Ancrod and 5 μl of tPA in TBS-T80, to initiate Pn generation. Final concentrations of S2251, UFH/ATH, Ancrod, and tPA were 0.4 mM, 0-2.1 U/ml, 0.6 U/ml and 0.563 nM respectively, in 1/3 diluted NPP. The change in absorbance was measured every 10 s for 2 hours at 405 nm and 450 nm in 37 °C. The Acorr

values were plotted against time squared to obtain initial Pn generation rates (s^{-1}) (refer to

Section 2.15.2 for calculation of Acorr and Pn generation rates).

2.11.1 Clot Lysis Time of the Fibrin Clot in the Presence of Anticoagulants

The clot lysis time was determined using the turbidity data (450 nm) from experiments

conducted in Section 2.11. Clot lysis time was defined as the time from Pn generation initiation

to the time when turbidity had decreased to half its maximal value.

2.11.2 Clot Lysis Time of the Fibrin Clot in Plasminogen Deficient Plasma with Added Glu-Plasminogen Titration

To further evaluate the effect of the anticoagulants on clot-lysis time, a high dose of ATH

(10 U/ml) was added to PgdP with increasing known concentrations of Glu-Pg. 90 μl of PgdP,

S2251, Glu-Pg and ATH was added to 5 μl of Ancrod and 5 μl of tPA to initiate Pn generation.

Final concentrations of S2251, Glu-Pg, ATH, Ancrod, and tPA were 0.4 mM, 0-3 μM, 10 U/ml,

0.6 U/ml, and 0.563 nM, respectively. Clot lysis time in the presence and absence of 10 U/ml of

ATH was compared at each concentration of Glu-Pg (0.4-3 μM).

2.12 Specific Activity of Plasmin against S2251 in Plasma for Continuous Plasmin Generation Kinetic Assay

To convert the change in absorbance (mOD/min), into Pn concentrations, in the

subsequent Pn generation experiments, various concentrations of Pn were incubated with S2251

in 1/3 diluted NPP in TSP. In brief, 90 μl of S2251 (0.44 mM) in NPP was added to 10 μl of Pn

(0-5 μM). The change in absorbance was measured at 37 °C, every 10 s for 1 hour at 405 nm

(S2251 cleavage) and 450 nm (turbidity change). Acorr was plotted against time and the initial

rate (mOD/min) of S2251 cleavage by Pn was determined for each Pn concentration (0-500 nM)

(refer to Section 2.15.3 for calculations). Initial linear rate (mOD/min) was plotted against corresponding Pn concentrations (0-500 nM) and fit to a linear trendline.

2.13 Optimization of tPA Concentration for Continuous Plasmin Generation Kinetic Assay in Plasma

To determine the optimal tPA concentration for the continuous Pn generation assay, 90 μl of NPP and S2251 in TSP was added to wells containing various concentrations of tPA to initiate Pn generation. Final concentrations of S2251 and tPA was 0.4 mM and 0-23.8 nM in 1/3 diluted NPP. Pn activity was monitored every 10 s for 3 hours at 405 and 450 nm in 37 °C.

2.14 Continuous Plasmin Generation Continuous Assay

Continuous Pn generation in the presence or absence of 5 U/ml ATH or UFH, in plasma was monitored over 2 hours. In brief, 90 μl consisting of NPP, S2251 ± UFH/ATH in TSP was added to wells containing 10 μl of tPA in TSP to initiate Pn generation. Final concentrations of S2251, ATH/UFH, and tPA at initiation were 0.4 mM, 5 U/ml, and 23.8 nM, respectively. Absorbance was measured at 37 °C every 10 s for 2 hours at 405 nm and 450 nm.

Acorr was plotted against time squared and the first derivative was extracted (Section 2.15.2). The AUC of the first derivative was calculated, which will be indicative of the Pn potential (Section 2.15.4 and 2.15.1).

2.15 Calculations and Statistical Analysis

All graphs were produced in Microsoft Excel 2010. Comparisons of the data were done using Minitab 13.32 in which One Way and Two Way ANOVA and t-tests were conducted. Tukey's HSD was used as the post hoc test. Values of $p < 0.05$ were deemed significant.

2.15.1 Area Under The Curve

Area under the curve between time points was calculated using the equation:

$$AUC = \left(\frac{y_{t_{x+1}} + y_{t_x}}{2}\right) \cdot (t_{x+1} - t_x)$$

$t = time\ (mins)$

$x = time\ points\ (0, 0.5, 1, 2, 5, 10, 20, and\ 60\ mins)$

$y = plasmin\ concentration\ (nM)$

The sum of the areas found between time points was taken to produce total area under the curve (AUC).

2.15.2 Corrected Absorbance (Acorr)

The absorbance of Pn specific activity or Pn generation was corrected as follows (previously described by Kim et al.) (81):

$$Acorr = A405 - (A450 \times CF)$$

$$CF = \frac{A405}{A450}\ in\ the\ absence\ of\ tPA\ (ratio\ reflecting\ the\ turbidity\ measured\ at\ A405)$$

$A405 = absorbance\ at\ 405nm\ (mOD)$

$A450 = absorbance\ at\ 450nm\ (mOD)$

2.15.3 Time Squared Analysis for Determining Initial Rates of Plasmin Generation

Similar calculations as found in Kim et al., were performed (81). Acorr was plotted against time squared to determine the rates of Pn generation according to the following relationship:

$$Acorr = \left(SA \times \frac{r}{2}\right) \times t^2$$

$SA = specific\ activity\ of\ Pn\ against\ S2251\ in\ the\ presence\ of\ a\ fibrin\ clot\ (Acorr$

$$\cdot min^{-1} \cdot nM^{-1})$$

$r = rate\ of\ Pn\ generation\ (s^{-1})$

$t = time\ (s)$

$$SA \times \frac{r}{2} = slope\ of\ Acorr\ vs.\ t^2\ (Acorr \cdot min^{-1} \cdot s^2)$$

In determining the slopes of Acorr versus time squared plots, the rate of Pn generation (r) can be determined with experimentally determined SA (Section 2.9 or 2.12), rearranging the slope equation above as follows:

$$r = \frac{(slope\ of\ Acorr\ vs.\ t^2) \times 2}{SA}$$

The r value is divided by tPA concentration to account for the dependence of rate on enzyme concentration.

2.15.4 Calculation of Plasmin Potential

In order to determine Pn potential of Pn generation experiments in the presence of 0 and 5 U/ml of UFH or ATH, raw data was corrected for turbidity as shown above. Acorr (OD) was plotted against time (s) in Microsoft Excel 2010 and exported to Table Curve Version 5.0.1. In Table Curve, a mathematical model was fitted to each set of data and exported back to Excel. This was done to eliminate any noise produced when measuring absorbance in the spectrophotometer, without compromising the trend observed in each condition. The first derivative (running average) was calculated as the slope between 3 points and plotted against time (s), for each fitted trend. The AUC for the data was calculated as previously described in Section 2.15.1, to determine the Pn potential.

3 Results

3.1 Plasmin Activity Standard Curve in Plasma

In order to convert absorbance values obtained from Pn generation experiments to Pn concentration, a Pn activity standard curve was produced. Increasing concentrations of purified Pn were plotted against absorbance produced with chromogenic substrate, S2251. The plot of the standard curve (Fig. 6) yielded a linear relationship between Pn concentration and absorbance, with a model of $y = 0.0132x + 0.05$ and $R^2 = 0.965$, thus showing that the increase in Pn concentration resulted in proportional increases in Pn activity against S2251.
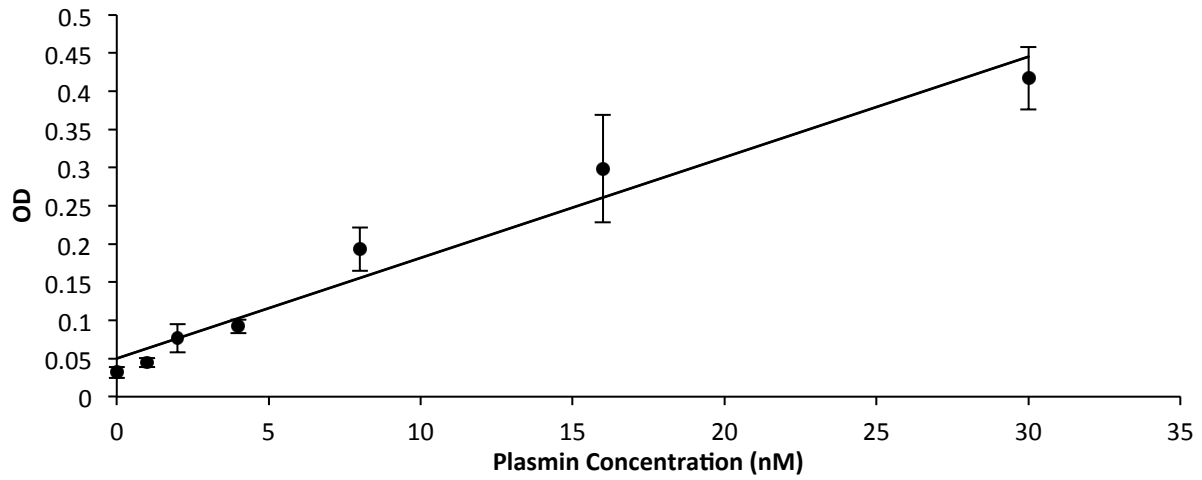
Figure 6. Plasmin Activity Standard Curve.

Various concentrations of purified Pn were incubated with excess S2251 in TSP. After 20 mins,

50% acetic acid was added to stop the reaction and absorbance was measured at 405 nm. Results

are mean ± SEM (n = 4).

3.2 Development of Assay for Plasmin Generation in Plasma

3.2.1 Testing for PAI-1, tPA, Fib activity against S2251

To ensure there was no activity of various components of the Pn generation assay against S2251 (used to quantify generated Pn), PAI-1, tPA, and Fib were incubated with S2251 and absorbance over time was measured at 405 nm. There was no observed difference between incubation of PAI-1 + S2251 and S2251 alone (Fig. 7). The slight difference seen between tPA+ Fib ± S2251 and S2251 alone was minimal when compared to the absorbance measured with 2.5 nM or 10 nM Pn + S2251 (Fig. 7).
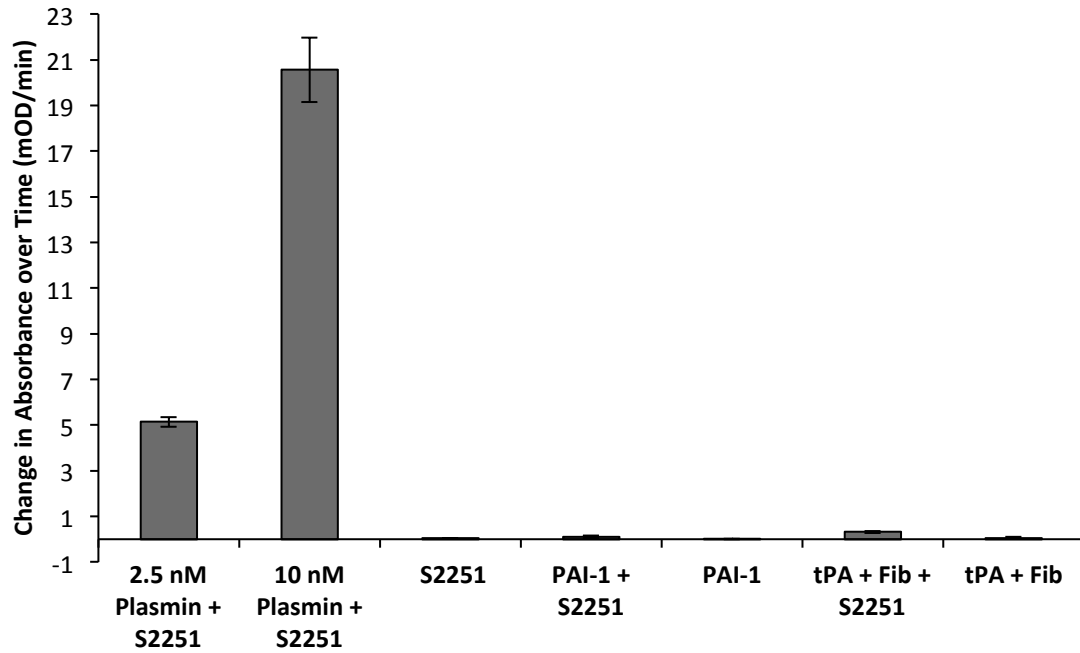
Figure 7. Testing PAI-1, tPA, and Fib interaction with S2251.

Change in absorbance over time from incubation of PAI-1 (44.64 nM) or tPA (89.25 nM) + Fib (150 μg/ml) ± S2251 (0.5 mM) was measured at 405 nm for 20 mins every 10 s. Results represent mean (n = 3) ± SEM.

3.2.2 Testing PAI-1 Inhibition of tPA

      To test the efficiency and the minimal time for PAI-1 inhibition of tPA, PAI-1 was allowed to incubate with tPA for 0-180 s and then added to NPP to measure if any Pn would be generated. The change in absorbance over time of Pn activity, due to possible residual tPA activity, was similar between all incubation times between 0-180 s (0 s was immediate addition of tPA and PAI-1 to NPP). There were no observed differences in tPA inhibition among all incubation times (Fig. 8).
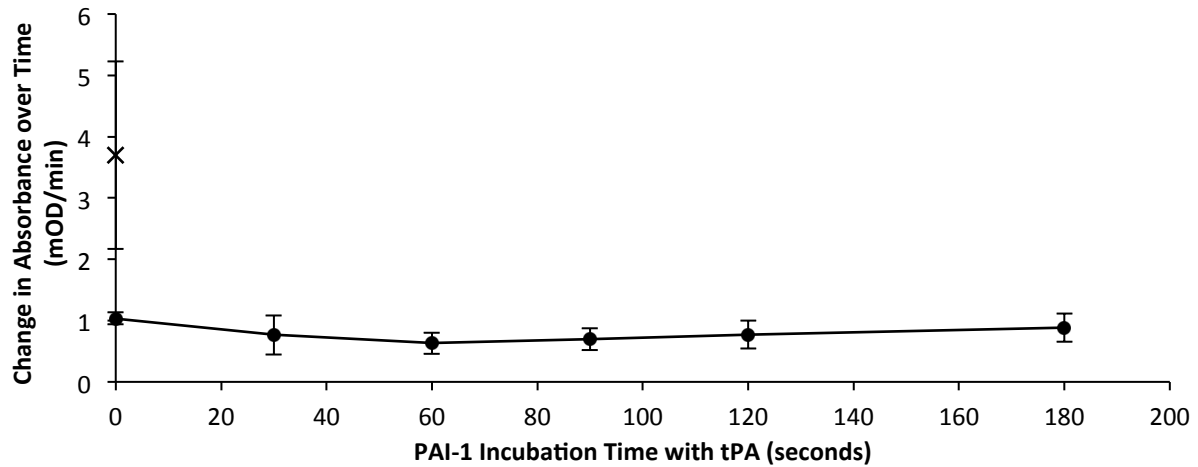
Figure 8. Testing for Minimal time for PAI-1 Inhibition of tPA.

PAI-1 was added to tPA, allowed to incubate for specified time periods, and added to NPP. Then, S2251 was added to detect any Pn produced from residual tPA activity. A control was conducted with the same components except in the absence of PAI-1 (×). Data are plotted as mean change in absorbance over time ± SEM (n = 3).

3.2.3 Plasmin Generation in Plasma using Various Concentrations of tPA and Fib

To find an optimal Pn generation curve, various combinations of tPA and Fib concentrations were compared in the Pn generation assay. There was minimal Pn generated when no Fib was added to the assay (Fig. 9: 4.464 nM tPA + 0 µg/ml Fib). For a given concentration of Fib, higher concentrations of tPA produced more Pn (Fig. 9). At 150 µg/ml of Fib both 8.928 and 4.464 nM tPA, did not result in large increases of Pn over 120 mins. At 600 µg/ml Fib, both 8.928 and 4.464 nM tPA produced the most Pn activity, however, absorbance values were above the value of the highest standard in the (Fig. 6). As well, these higher absorbance values may not be accurate indices of Pn concentration as high Pn concentrations can consume all/most S2251 in the assay. The intermediate Pn generation curve using 8.928 nM tPA and 300 µg/ml Fib allowed for a steady increase in Pn that fell within the standard curve and eliminated the inaccuracies from complete consumption of S2251.
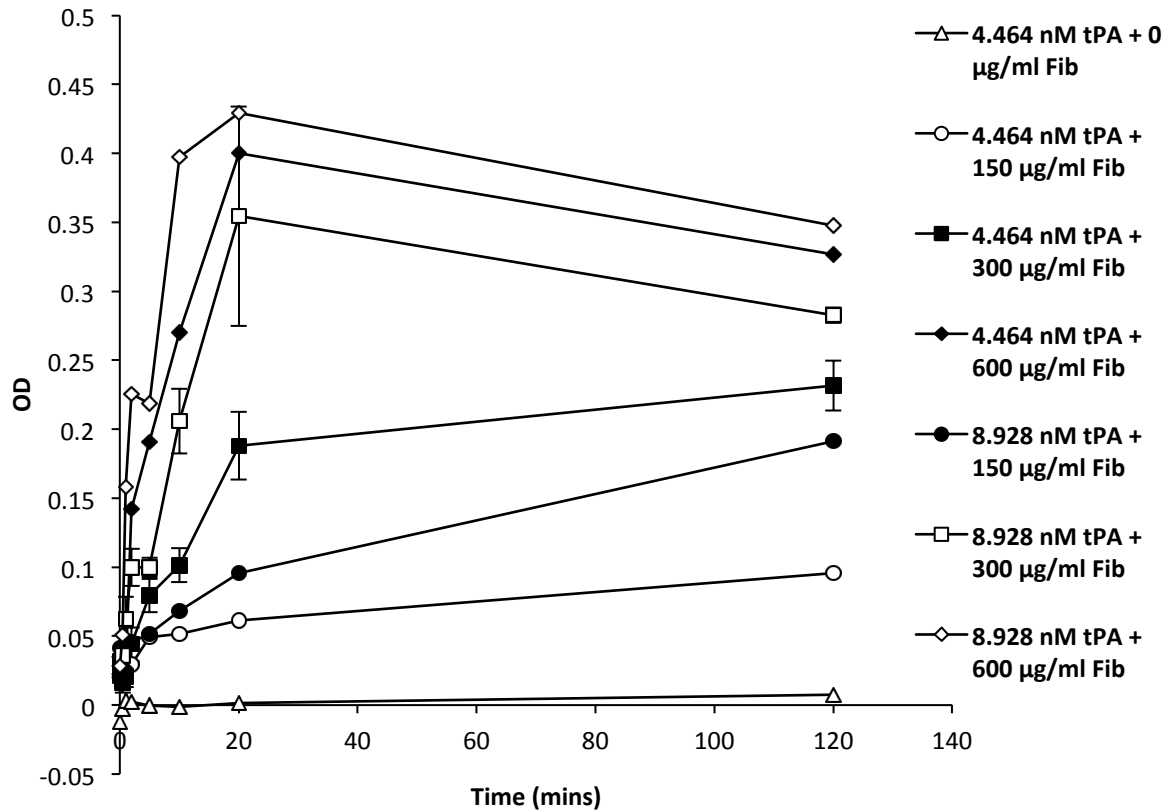
Figure 9. Testing Various tPA and Fib concentrations for Optimal Plasmin Generation Assay.

Different combintations of tPA and Fib concentrations in TSP were added to NPP to initiate Pn generation. Absorbance values are plotted at 405 nm. Results for 8.928 nM tPA + 300 µg/ml Fib are mean (n = 4) ± SEM and 4.464 nM tPA + 300 µg/ml Fib are mean (n = 3) ± SEM. Remaining conditions are n = 1.

3.3 Optimization of Plasmin Generation Assay in Absence of Anticoagulants

Pn generation was conducted in the absence of anticoagulants, to observe the overall Pn generation profile over time. As well, the experiments were conducted weekly, to ensure consistency of the assay system before testing in the presence of UFH, LMWH, and ATH. At 0, 0.5, and 1 min mean absorbance was similar at 0.043 ± 0.007, 0.0405 ± 0.008, and 0.0485 ± 0.010, respectively (Fig. 10). The largest increase in Pn generation was between 1 min and 20 mins (0.0485 ± 0.010 to 0.298 ± 0.016). After 20 mins, Pn generation did not increase greatly as absorbance was 0.319 ± 0.019 at 60 mins. This was deemed as an optimal curve as it allowed for the gradual increase in Pn concentration over a reasonable experimental time frame. The gradual increase in Pn concentration, over time, will allow for better insight into the effect of the anticoagulants to the rate of Pn generation.
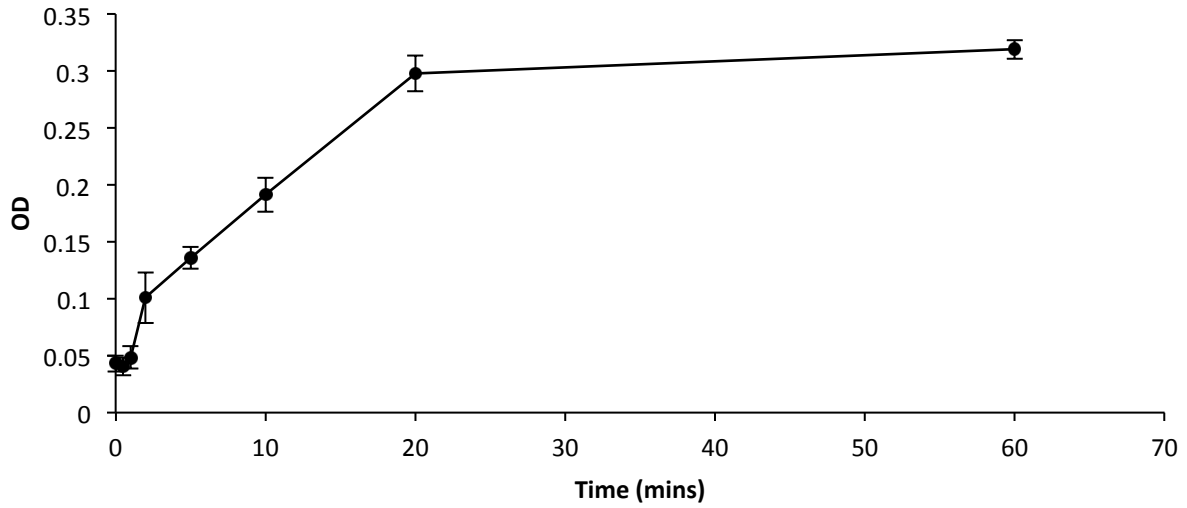
Figure 10. Plasmin Generation Over Time in the Absence of Anticoagulants.

tPA and Fib in TSP was added to NPP to initiate Pn generation. Subsamples were removed at the

indicated time points and incubated with PAI-1 to inhibit further Pn generation. Mean

absorbance (n = 6) ± SEM, due to Pn activity against S2251 was plotted against time.

3.4 Plasmin Generation in Plasma Over Time in the Presence of UFH, LMWH, and ATH

To test the effects of anticoagulants on Pn generation, experiments were conducted as previously described, in the presence of increasing doses of UFH, LMWH, and ATH. When observing the Pn generation profile over time, for each anticoagulant, there did not appear to be a dose dependent response (Fig. 11 A, B and C). However, there may be a slight decrease in Pn generation when comparing the curves with and without UFH and ATH, but not LMWH at any dose.

The AUC is a quantity that can be used as an overall measure of Pn generation. There was no clear dose dependent relationship between the AUC and various doses of UFH, LMWH, and ATH (Fig. 12 A, B and C). However, there was a significant decrease in AUC for UFH and ATH at 0.7 U/ml as well as 2.1 U/ml for ATH only ($p = 0.019$ and $p = 0.001$) (Fig. 12 A and C). This indicates increased Pn inhibition in the presence of UFH and ATH.

When comparing differences between anticoagulants at each specific dose (Fig. 13 A, B, C and D), it was found that at 0.7 U/ml, Pn generation inhibition was significantly higher in the presence of ATH (23928.79 ± 2931.70 nM•min) when compared to LMWH (36956.06 ± 2192.19 nM•min) ($p = 0.010$) (Fig. 13 B). At 1.4 U/ml there was significantly more Pn inhibition in the presence of UFH (30628.22 ± 2059.42 nM•min) and ATH (30150.19 ± 1035.88 nM•min) when compared to LMWH (38041.57 ± 1671.10 nM•min) ($p = 0.009$) (Fig. 13 C). At the highest doses tested, 2.1 U/ml, ATH significantly decreased overall Pn generation (26914.87 ± 1483.87 nM•min) in comparison to LMWH (32344.03 ± 1462.90 nM•min) ($p = 0.032$) (Fig. 13 D). Lastly, there was no statistical difference in Pn generation between UFH and ATH at any dose.
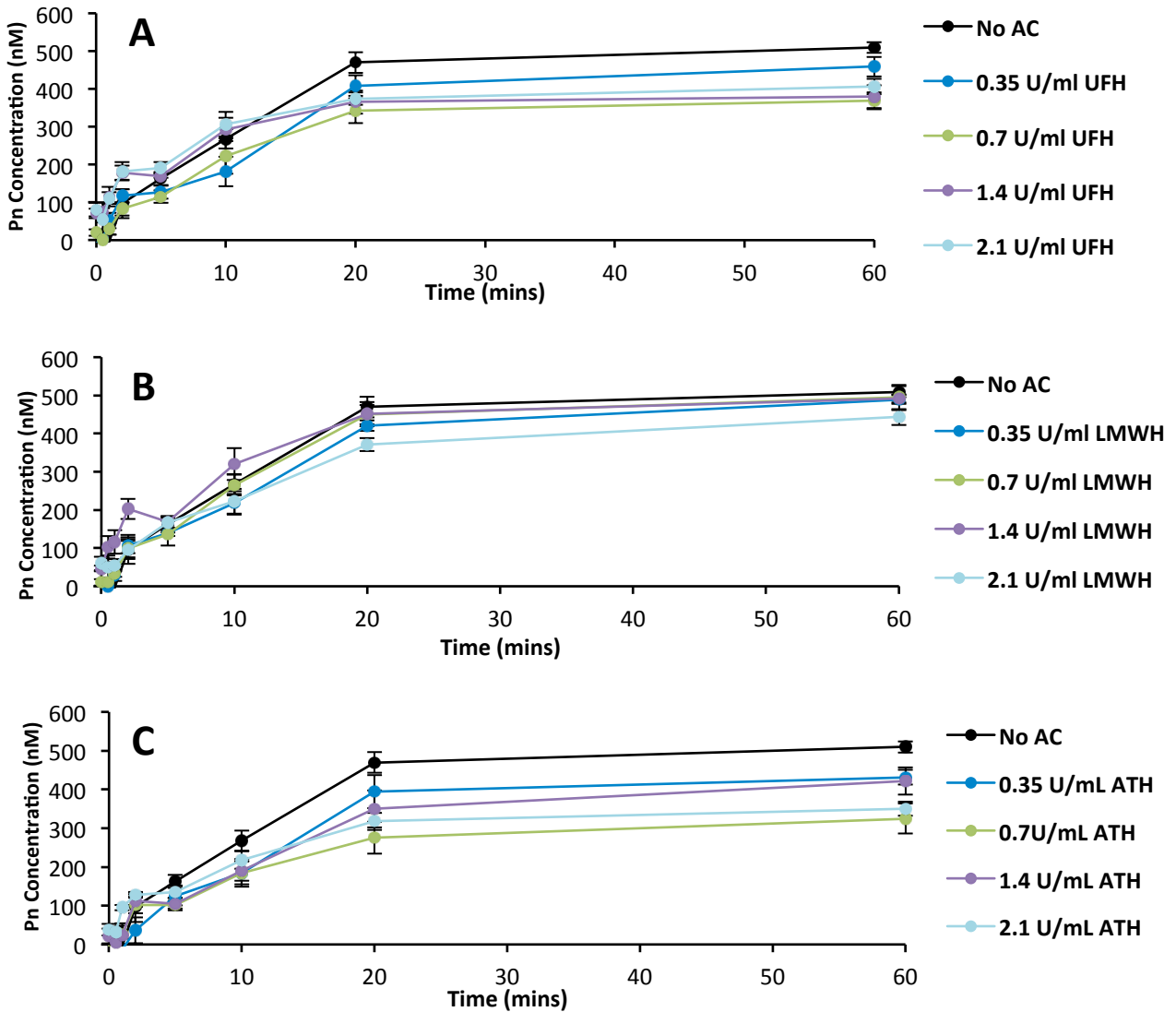
Figure 11. Comparison of the Effect of Different Anticoagulant Doses on Plasmin Generation Over Time.

tPA and Fib in TSP was added to NPP ± various doses of UFH (A), LMWH (B) or ATH (C) to initiate Pn generation. Subsamples were removed at the indicated time points and incubated with PAI-1 to inhibit further Pn generation. The concentration of active Pn generated at various times was quantified (as described in Fig. 6) and adjusted to 100% plasma. Results for each anticoagulant (A B C) was compared against the absence of anticoagulants (No AC) plotted as mean (n = 5) ± SEM.
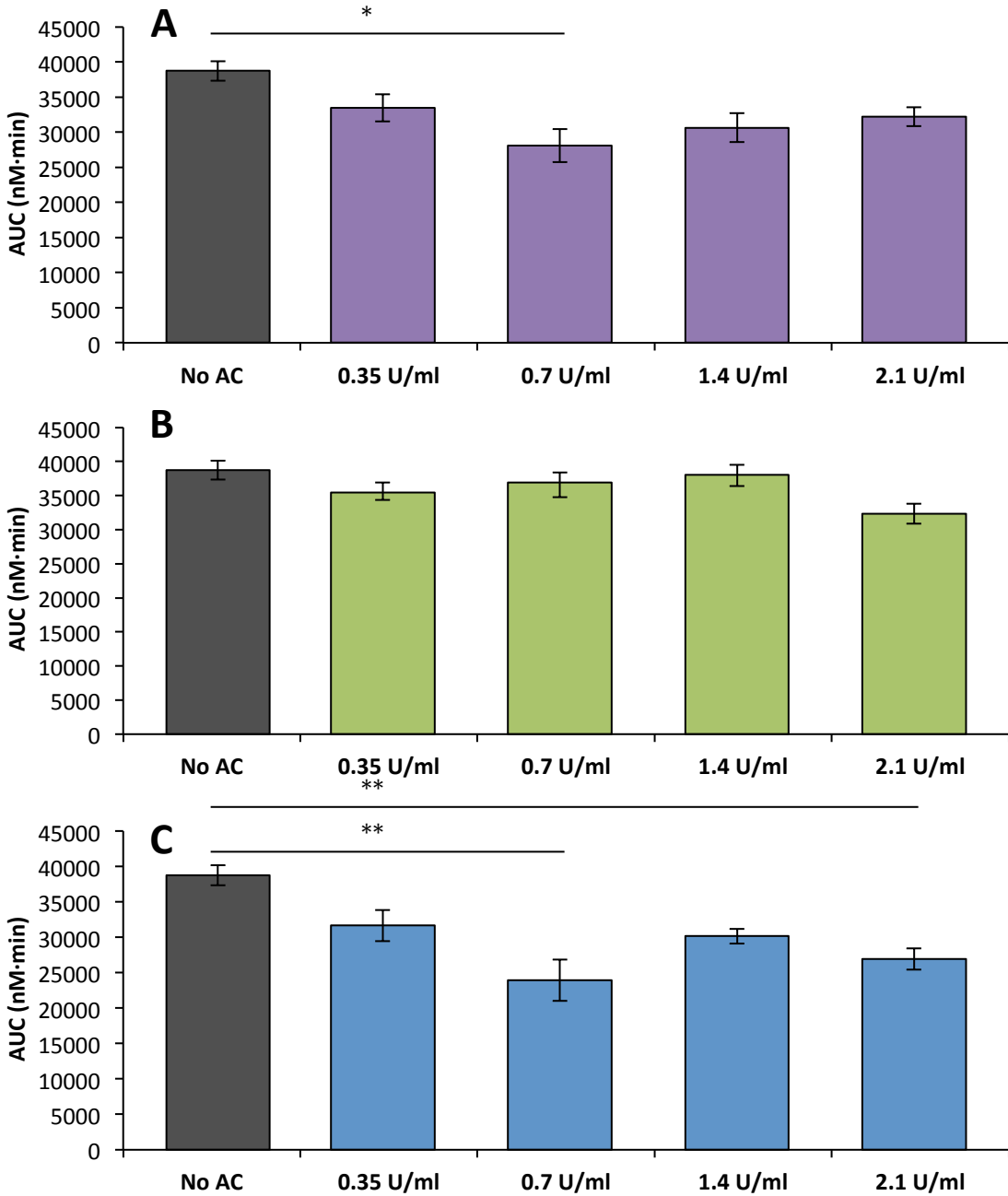
Figure 12. AUC Comparison of the Effect of Dose on Overall Plasmin Generation.

AUC was calculated for the curves in Fig. 11, as described in Section 2.15.1. Each anticoagulant:

UFH (A), LMWH (B), and ATH (C) was compared against the absence of anticoagulants (No

AC). Data is expressed as mean (n = 5) ± SEM (*p = 0.019, **p = 0.001).
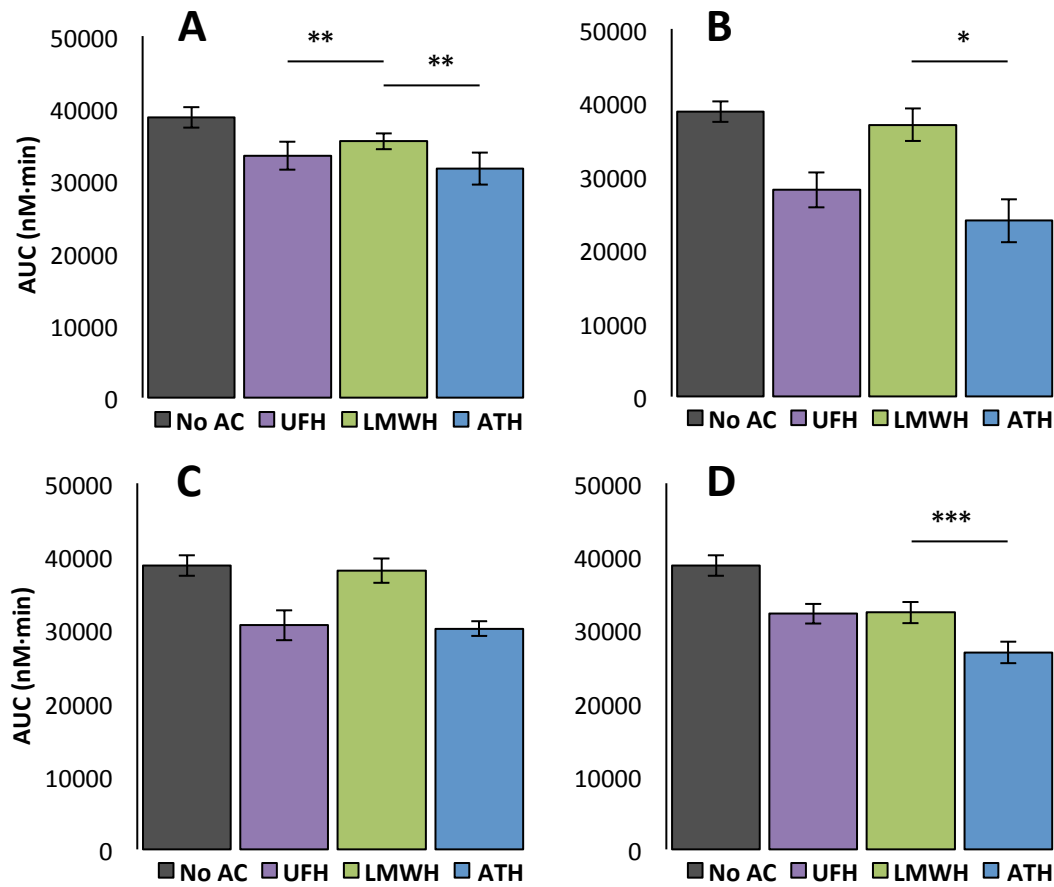
Figure 13. AUC Comparison of the Effect of Different Anticoagulants on Overall Plasmin Generation.

tPA and Fib in TSP was added to NPP ± UFH, LMWH, or ATH at 0.35 U/ml (A), 0.7 U/ml (B), 1.4 U/ml (C), 2.1 U/ml (D) to initiate Pn generation. Subsamples were removed at various time points from 0-60 mins and incubated with PAI-1 to inhibit further Pn generation. Mean AUC at each dose was compared between UFH (purple bars), LMWH (green bars), and ATH (blue bars) (n = 5 ± SEM). Absence of anticoagulants (black bars) represents the same data set (mean with n = 5 ± SEM) (*p = 0.010, **p = 0.009, ***p = 0.032).

3.4.1 Testing for Dose Dependent Response

To clarify the dose-dependent relationship between AUC and anticoagulants, lower doses of ATH were used, and Pn generation experiments were conducted as previously described (Section 2.5). When observing the Pn generation profile over time, for each dose of ATH (0.001-0.1 U/ml) there was no significant dose dependent response observed (Fig. 14). Highest Pn concentration generated (at 60 mins) for 0.001 U/ml (lowest dose tested) and 0.1 U/ml (highest dose tested) were 447.601 ± 66.155 nM and 391.098 ± 50.189 nM, respectively.

The AUC for the same set of Pn generation experiments with lowered doses of ATH did not show a definitive relationship with decreasing doses (0.1-0.001 U/ml) (Fig. 15). There were minimal differences in AUC between the lowest and highest dose (0.001 U/ml and 0.1 U/ml) and the absence of anticoagulants (No AC) with AUCs of 33809.8171 ± 5679.856, 27790.9561 ± 4271.543, and 38736.1631 ± 1397.128 nM•min respectively. There was also no difference in AUC in the absence of anticoagulants compared to that of a control in which TSP was added to NPP instead of ATH, before initiation of Pn generation (Fig. 15). This indicated that previous observed decrease in AUC was due to the presence of anticoagulants and not from any dilution factor caused when adding the anticoagulants.

3.4.2 Plasmin Generation in Plasminogen Deficient Plasma

Pn generation was conducted with PgdP in place of NPP to confirm that absorbance measured was due to the Pn generated in the experiment. As expected, there was no Pn quantified with the replacement of NPP with PgdP, as shown in Fig. 14.
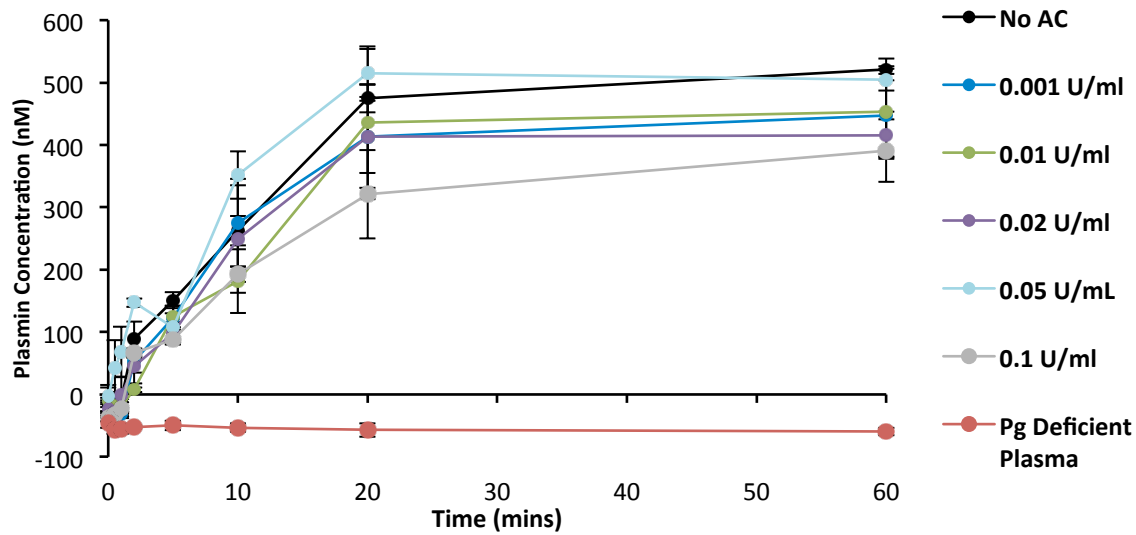
Figure 14. Testing the Effect of Lower Doses of ATH on Plasmin Generation.

tPA and Fib in TSP were added to NPP or PgdP (red circles) ± ATH at various doses to initiate

Pn generation. Subsamples were removed at the indicated time points and incubated with PAI-1

to inhibit further Pn generation. The concentration of active Pn generated at the various times

was quantified as described in Fig. 6 and adjusted to 100% plasma. Lower doses of ATH are

plotted as mean (n = 3) ± SEM, except 0.1 U/ml (n = 2) ± range. The absence of anticoagulants

(No AC) is plotted as mean (n = 9) ± SEM.
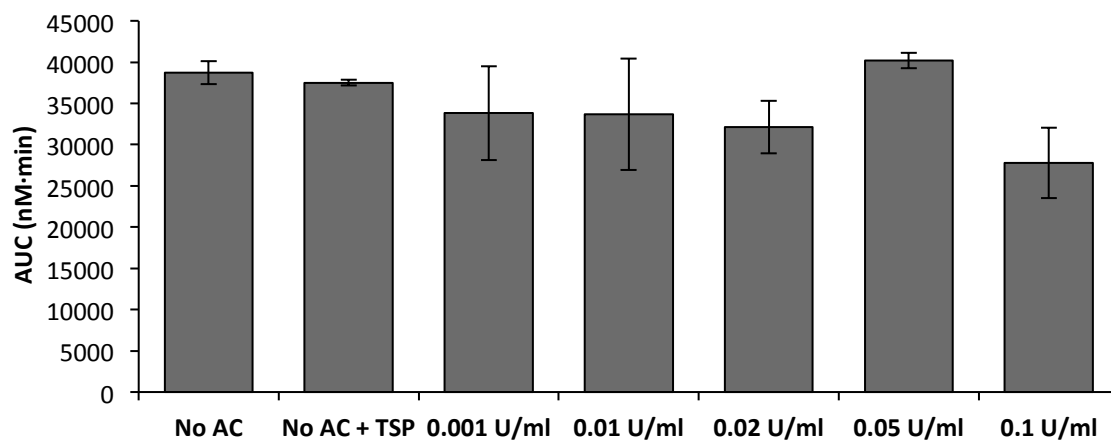
Figure 15. AUC Comparison of the Effect of Lower Doses of ATH on Plasmin Generation.

AUC was calculated for curves in Fig. 14, as described in Calculations & Statistical Analysis (Section 2.15). Results are mean (n = 3) ± SEM, except 0.1 U/ml (n = 2) ± range and absence of anticoagulants (No AC) represents mean (n = 9) ± SEM.

3.5 Quantification of PAM Complexes

3.5.1 Testing for Soybean Trypsin Inhibitor Effectiveness on Plasmin

The effectiveness of SBTI inhibition of Pn was tested by quantifying Pn activity with S2251 after incubation of Pn, PAM, and α_2-M with PAI-1 ± SBTI (Fig. 16). It was observed that SBTI inhibited free Pn (Pn + PAI-1 + SBTI, Pn + SBTI) but not α_2-M-bound Pn (PAM + PAI-1 + SBTI versus PAM + PAI-1). PAI-1, SBTI, and α_2-M had minimal effect on the Pn specific chromogenic substrate, S2251.
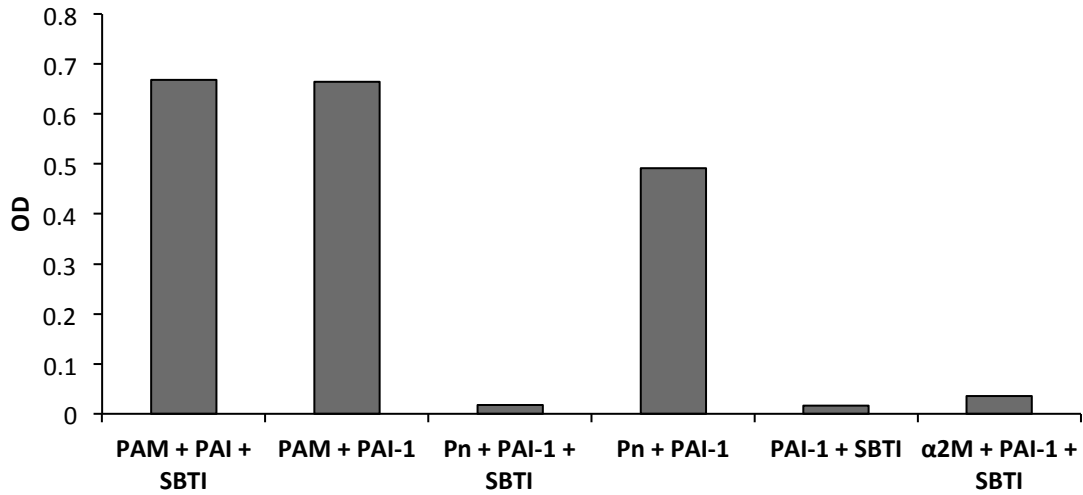
Figure 16. Testing for SBTI Effectiveness on Free Plasmin.

Purified PAM, Pn, or α_2-M was incubated for 2 mins with excess PAI-1 + SBTI, PAI-1 or SBTI only, to allow for free Pn inhibition. Pn specific substrate, S2251, was added and chromogenic activity stopped after 20 mins with the addition of 50% acetic acid. Results are absorbance measured at 405 nm (n = 1), representing remaining Pn chromogenic activity.

3.5.2 Change in Concentration of PAM Complexes During Plasmin Generation

PAM complexes were quantified using SBTI to inhibit free Pn and remaining Pn activity measured with S2251, which is reflective of Pn bound to α_2-M (PAM). This was done in the presence and absence of UFH or ATH (at various doses). Fig. 17 A shows a comparison of total Pn activity over time (data taken from Fig. 11) and the Pn activity attributable to PAM. The difference between the graphs represents free Pn. During Pn generation without anticoagulants, PAM concentration starts at -34.72 ± 6.59 nM and increases to 116.16 ± 0.79 nM (by 10 mins) and 459.60 ± 26.70 nM (at 20 mins). Eventually, the majority of the Pn is inhibited by α_2-M, as indicated by the convergence of the total Pn and PAM graphs at 60 mins.

Fig. 17 B and C compares PAM concentration during Pn generation over time, only, in the presence and absence of UFH or ATH at 0.35 U/ml and 0.7 U/ml. The graphs of total Pn generated over time at these doses (not shown) were similar to those shown in Fig. 11. There is a slight decrease in PAM at 20 and 60 mins when both UFH and ATH (at both doses) are present, when compared to their absence (Fig. 17 B and C), but not at 10 mins.

There was no significant difference in the AUCs of PAM generation curves between the absence of anticoagulants (36367.80 ± 1243.03 nM•min) and UFH or ATH at 0.35 U/ml (27935.61 ± 2006.6, 32591.54 ± 2309.89 nM•min) or 0.7 U/ml of UFH (31568.81 ± 2608.447 nM•min) ($p = 0.0655$) (Fig. 18). However at 0.7 U/ml ATH (27547.35 ± 1962.80 nM•min), there was a significant reduction in PAM complexes formed in comparison to the absence of anticoagulants ($p = 0.0426$) (Fig. 18). There were no differences in the AUC of PAM complexes between UFH and ATH at any dose ($p = 0.0655$).
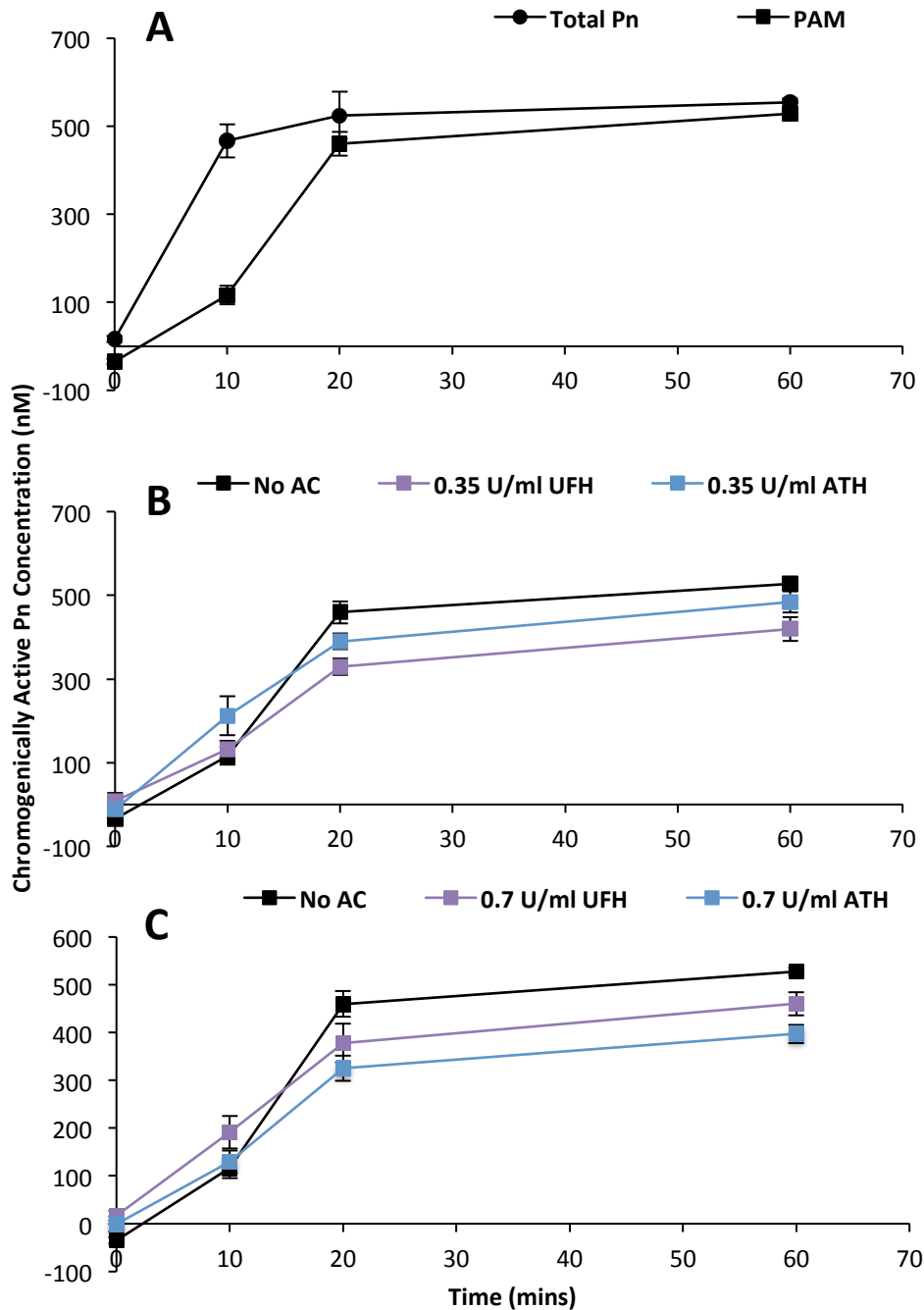
Figure 17. Quantification of PAM Complexes during Plasmin Generation.

(A) Pn generation was conducted as described in Fig. 11, with modifications. In brief, tPA and

Fib in TSP was added to NPP to initiate Pn generation. Subsamples were removed at each

indicated time point and added to PAI-1 only (circles) or PAI-1 + SBTI (squares). The

concentration of Pn was quantified as described in Fig. 6 and represents total active Pn and

PAM, respectively. Similar experiments were conducted ± 0.35 U/ml (B) or 0.7 U/ml (C) of

UFH or ATH. The presence and absence of anticoagulants are plotted as mean (n = 3) ± SEM.
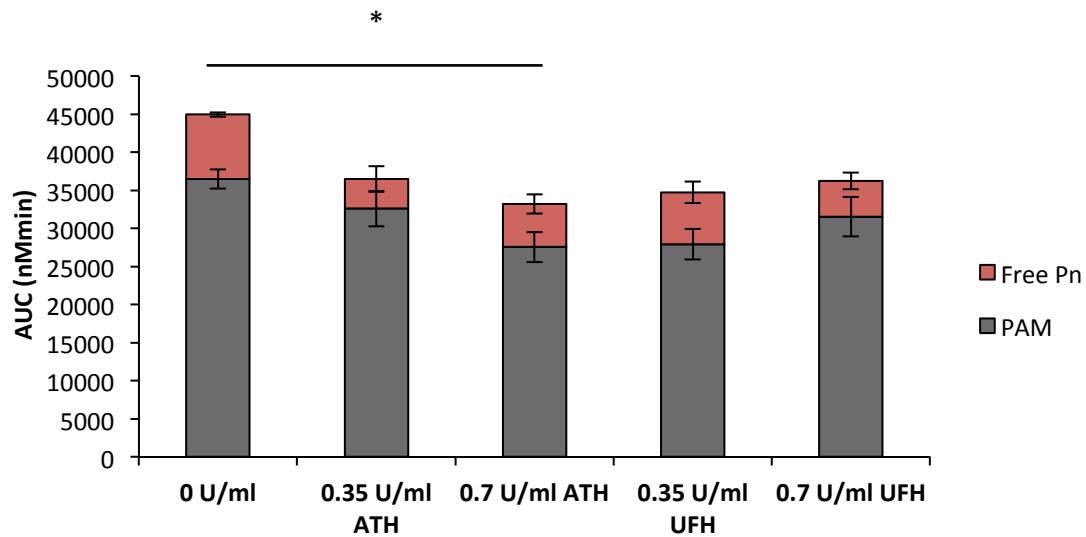
Figure 18. Comparison of the AUCs of PAM Complexes Formed during Plasmin Generation.

AUC was calculated for the graphs representing PAM complexes in Fig. 17, as described in Section 2.15. Total Pn AUC is shown as the sum of free Pn (red) and PAM complexes (grey). The PAM complex AUCs in the presence of UFH and ATH at both doses were compared to the absence of anticoagulant (No AC) (mean n = 3 ± SEM) (*p = 0.046).

3.6 Quantification of PAP Complexes with the Technozym PAP ELISA Kit

3.6.1 Technozym PAP ELISA Standard Curve

  To convert absorbance values (OD) obtained from the PAP ELISA to PAP concentrations, a standard curve was conducted with each ELISA using PAP complex standards provided by the kit. Fig. 19 depicts a typical standard curve resulting in a linear relationship between PAP concentration and absorbance with a model of $y = 0.0043x + 0.0021$ and $R^2 = 0.99872$.
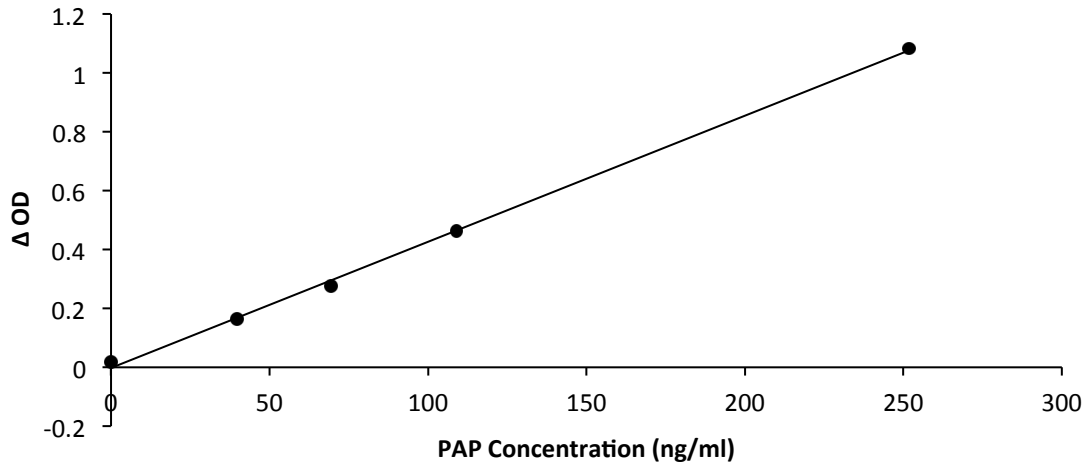
Figure 19. Technozym PAP ELISA Standard Curve.

Various concentrations of PAP complexes were measured using the ELISA method supplied by

the manufacturer. Corresponding absorbances were plotted against known PAP concentrations

(ng/ml) and fit to a linear trendline (solid). The equation of the line was used to convert

absorbance values into PAP concentrations found in Pn generation subsamples tested in the same

ELISA.

3.6.2 Specificity of the Technozym PAP ELISA Kit

Several controls were tested to ensure the Technozym PAP ELISA kit was only specific to PAP complexes and that UFH or ATH did not affect the sensitivity of the kit. The concentrations of reagents were selected to resemble corresponding amounts that are expected to be found in Pn generation subsamples. PAM complexes (2000 nM), Pn (1000 nM), UFH/ATH in NPP (0.7 U/ml), and NPP did not produce significant signal when compared to the high and how PAP calibrators provided by the kit (Fig. 20).
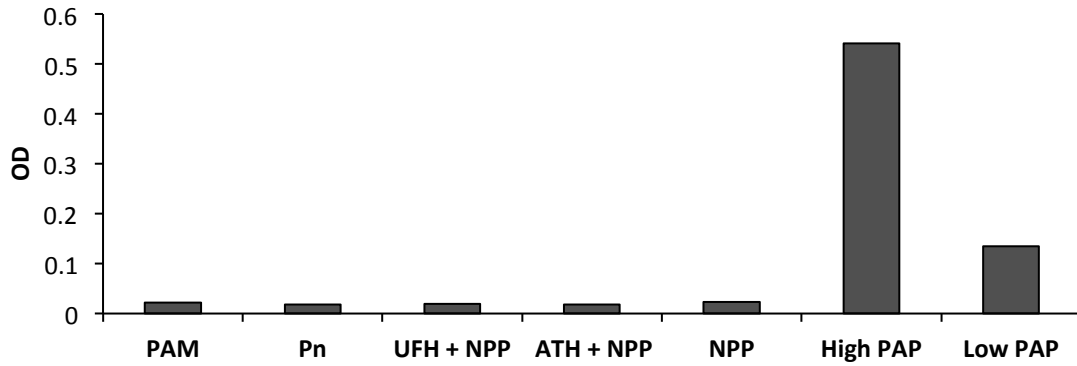
Figure 20. Testing for Specificity of Technozym PAP ELISA Kit.

PAM (2000 nM), Pn (1000 nM), 0.7 U/ml UFH/ATH + NPP, and NPP alone, were diluted

1:1000 and tested with ELISA. High and low PAP calibrators (0.85 nM and 0.22 nM,

respectively) provided by the ELISA manufacturer were used as a comparison (n = 1).

3.6.3 Quantification of PAP Complex Formation During Plasmin Generation with the Technozym PAP ELISA

Independent of the presence or absence of anticoagulants, the PAP complex formation profile over time had a general trend. PAP complexes were minimal at the start of Pn generation. The highest increase in PAP complexes occurred between 0 to 10 mins, going from 0 to approximately 1200 nM. There was no difference in the total amount of PAP complexes formed between this time frame in the presence and absence of anticoagulants ($p = 0.432$). From 10 to 20 mins, PAP concentrations increased slightly to approximately 1200-1400 nM. From 20 mins onwards, there was a slight increase in PAP concentrations (Fig. 21). There was no effect of anticoagulants on total PAP complex formation during Pn generation (at 60 mins) ($p = 0.544$).
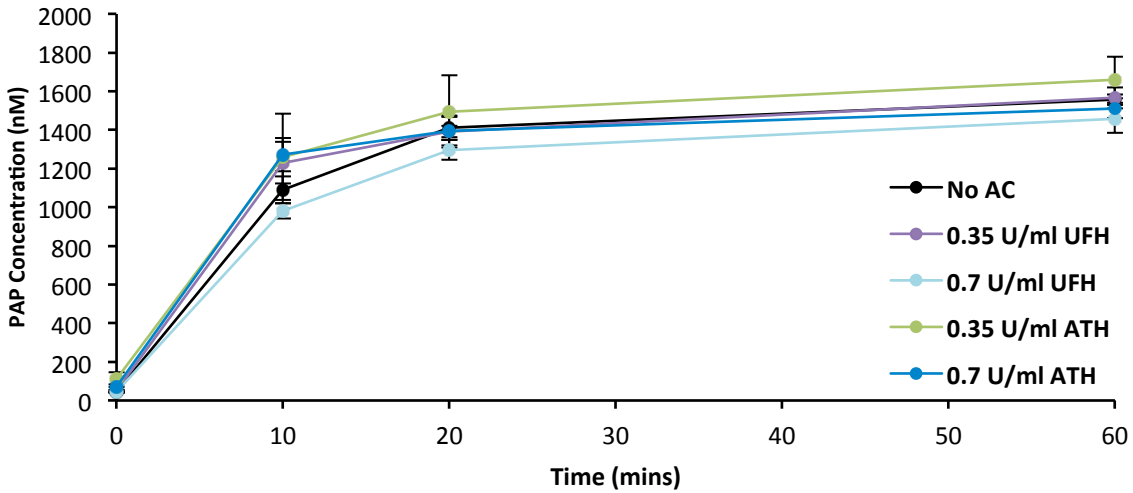
Figure 21. Quantification of PAP Complexes During Plasmin Generation in Plasma.

Subsamples taken from previously conducted Pn generation experiments were diluted 1:1000 in dilution buffer and quantified for PAP complexes were quantified by ELISA. The PAP complex concentrations generated at indicated time points (during Pn generation) in the presence of 0.35 U/ml and 0.7 U/ml UFH or ATH were compared to PAP complexes generated in the absence of anticoagulants (No AC). Results are mean (n = 3) ± SEM and adjusted for 100% plasma.

3.7 Quantification of Plasminogen Consumption with the Technozym ELISA Kit

3.7.1 Technozym Plasminogen ELISA Kit Standard Curve

Pg standards provided by the manufacturer were tested with each ELISA. An example of a typical standard curve is shown in Fig. 22. Log of the absorbance versus log of Pg concentration was graphed and data fit to a linear trendline with the equation y = 0.6118x + 0.1594 and R^2 of 0.9978.
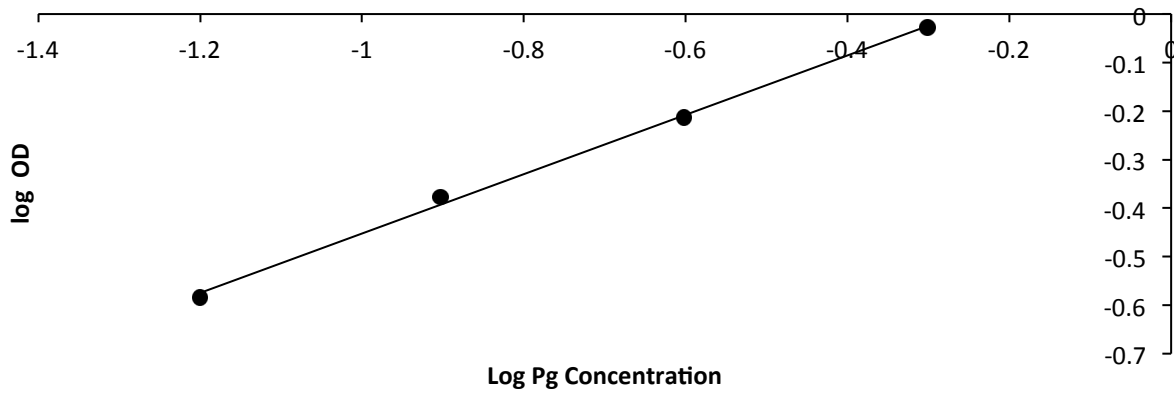
Figure 22. Technozym Plasminogen ELISA Log Standard Curve.

Pg standards (provided by the ELISA manufacturer) were tested with each ELISA. Log

absorbance at 450 nm was plotted against Log of Pg concentration. A linear trendline (solid line)

was fit and used to convert the absorbances of Pn generation samples to Pg concentrations.

3.7.2 Testing for Specificity and Accuracy of the Technozym Plasminogen ELISA Kit

Pg standards were tested along with purified Glu-Pg of similar concentrations. As expected, absorbance values of standards were similar to that of purified Glu-Pg at every concentration (Fig. 23 A). ATH at 2.1 U/ml in NPP (119.75 μg/ml) may have interfered slightly with Pg quantification compared to NPP alone (137.62 μg/ml) (Fig. 23 B). This was similarly seen with 0.7 U/ml of ATH in NPP (94.71 μg/ml) compared to the absence of ATH (124.05 μg/ml) (Fig. 23 C). UFH did not have an effect on Pg quantification when compared to NPP (Fig. 23 B). There was no Pg quantified in PgdP and the kit did not cross react with Pn (Fig. 23 C).
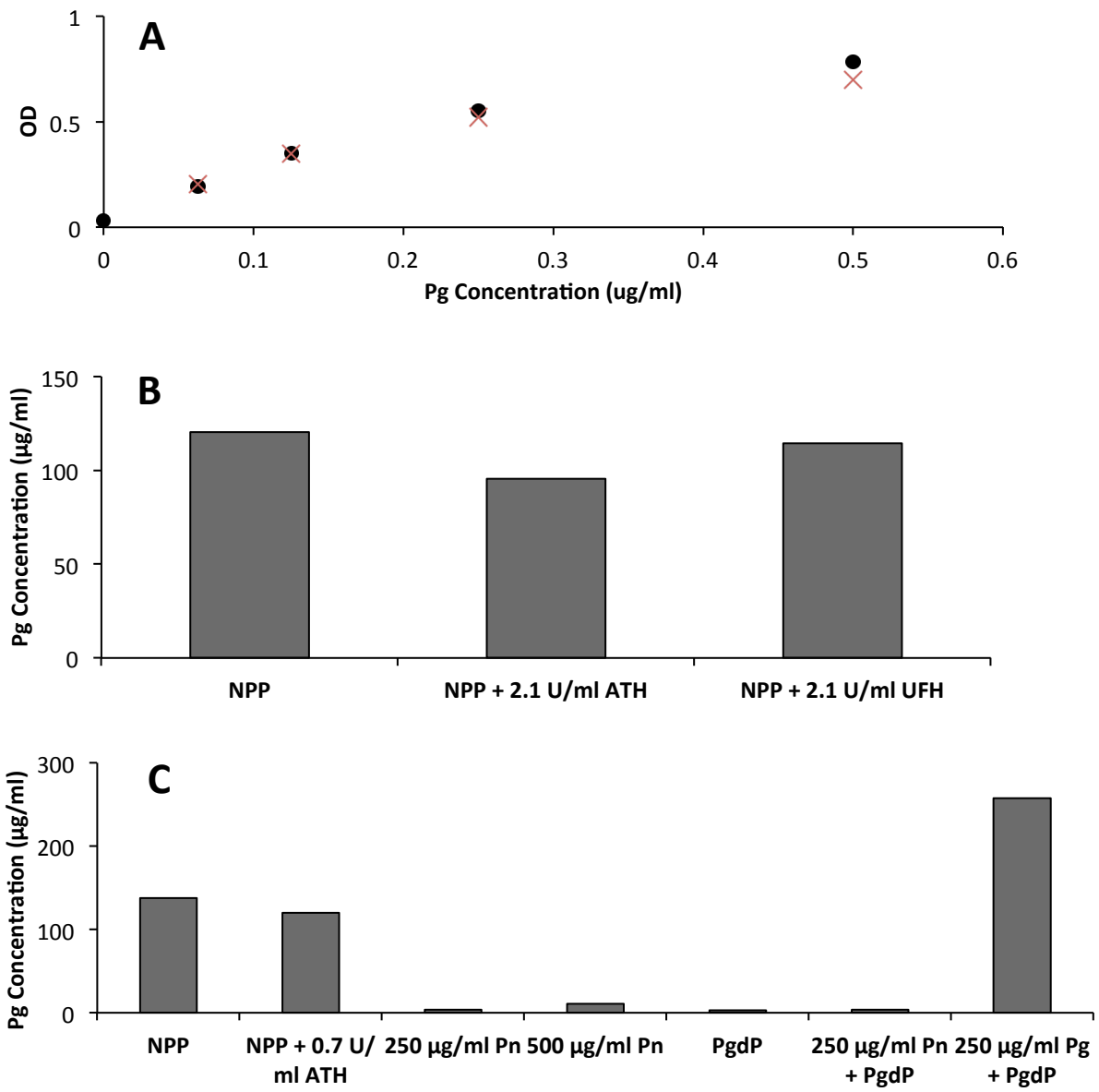
Figure 23. Testing for Specificity of Technozym Plasminogen ELISA Kit.

(A) Various concentrations of Pg were tested in ELISA kit. Pg standards provided by the manufacturer (×) were plotted against absorbance. The same concentrations of purified Glu-Pg were quantified by ELISA (black circles) and compared to the standards. (B C) Several other controls including NPP, UFH/ATH + NPP, Pn, and PgDP, were used to test the specificity of the ELISA Kit (bar graphs). Controls are n = 1, assayed in duplicate.

3.7.3 Quantifying Plasminogen Consumption During Plasmin Generation with the Technozym Plasminogen ELISA Kit

A general trend was observed for Pg consumption during Pn generation. Pg concentrations were between 500 and 600 nM for all conditions at the beginning of the Pn generation. The largest decrease in Pg was observed between 0 and 10 mins, to approximately 200 nM. There was no difference in the amount of Pg consumed between this time frame in the presence or absence of anticoagulants ($p = 0.067$). After 10 mins, the rate of Pg consumption decreased and from 20 to 60 mins, there was no further Pg consumption observed (Fig. 24). There were no differences in the total Pg consumed during Pn generation in the presence and absence of anticoagulants. ($p = 0.391$).
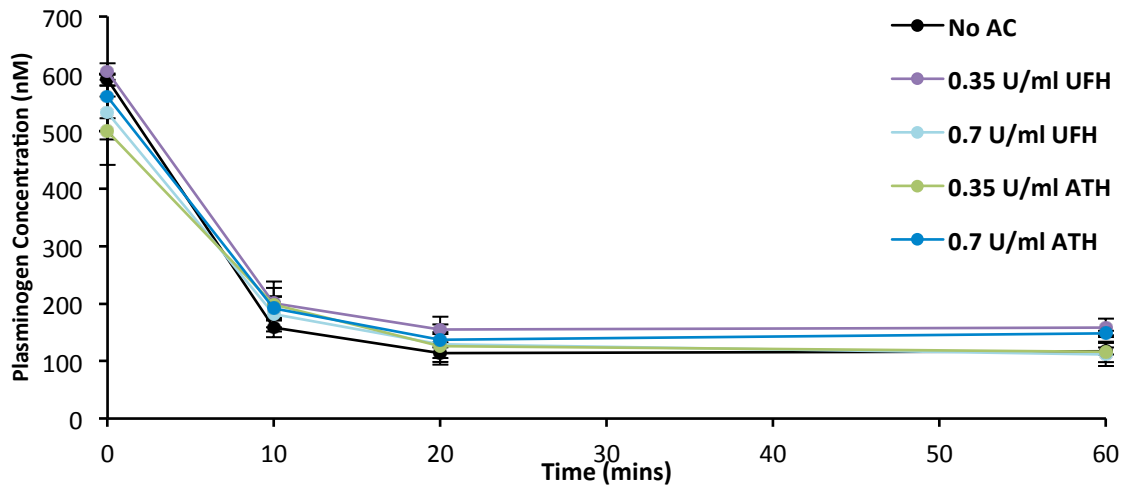
Figure 24. Quantification of Plasminogen Consumption During Plasmin Generation.

Subsamples stored from previous Pn generation experiments were diluted 1:1000 and tested with

the Technozym Pg ELISA. Results are n = 3 ± SEM, adjusted for 100% plasma.

3.8. Kinetics of Plasmin Generation in Plasma on a Fibrin Clot

In an effort to confirm the observations found in the previous Pn generation assays (±

UFH/LMWH/ATH) in Section 3.4, a more sensitive continuous Pn generation assay was

conducted on fibrin clots (in plasma) in the presence and absence of UFH and ATH (at similar

doses). This assay was adapted from past studies by Chander et al (9).

3.8.1 Specific Activity of Plasmin against S2251 in Plasma on a Fibrin Clot

Various concentrations of Pn were incubated with fixed amounts of S2251, in the

presence of Ancrod. The rate of substrate cleavage (change in absorbance over time, mOD/min)

was plotted against corresponding Pn concentration (nM) in 100% NPP. Pn activity was minimal

at concentrations lower than 900 nM due to α_2-AP (with a plasma concentration of

approximately 1000 nM) inhibition of Pn, as expected (Fig. 25) (54). At concentrations above

1000 nM, Pn activity against S2251 increased linearly with increasing Pn concentration (Fig.

25). Rate of substrate cleavage (mOD/min) of Pn concentrations above 1000 nM plotted against

Pn concentrations (adjusted for 100% plasma) yielded a linear model of $y = 2.119x - 2315.6$

with $R^2 = 0.85061$. The SA of Pn was 2.119 mOD/min/nM (slope of the linear equation).
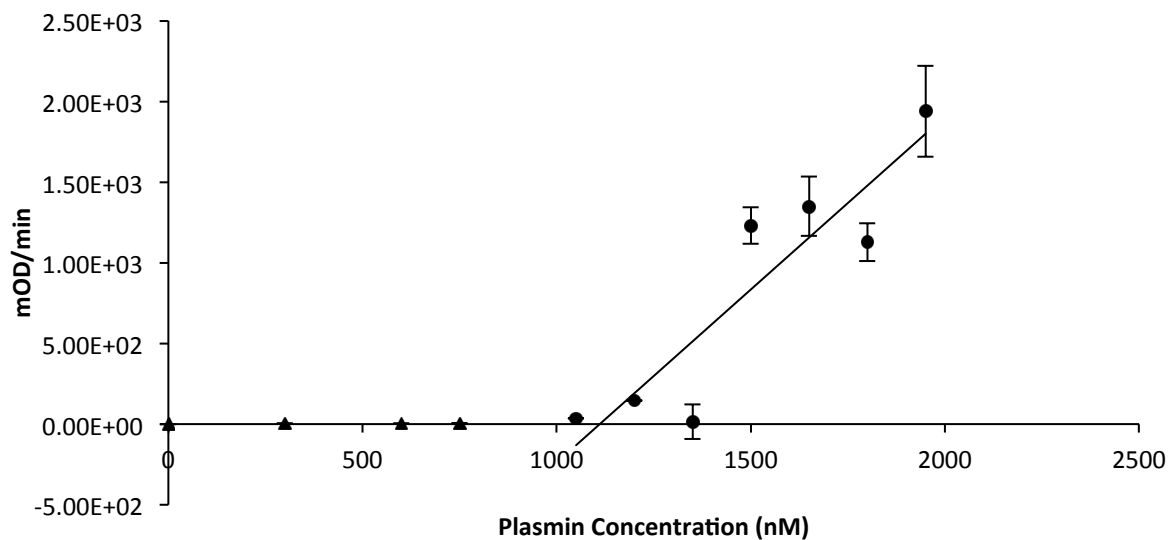
Figure 25. Specific Activity of Plasmin in Plasma on a Fibrin Clot.

Various concentrations of Pn were incubated with S2251 in 1/3 diluted NPP in the presence of

Ancrod. Pn activity was quantified by measuring change in absorbance over time, indicative of

S2251 cleavage on a fibrin clot. Mean change in absorbance over time (mOD/min) was corrected

for turbidity and plotted against corresponding Pn concentrations (0-2000 nM) (n = 3 ± SEM for

concentrations above 1000 nM Pn (circles), n = 2 ± range for concentrations below 1000 nM Pn

(triangles). A linear trendline (solid line) was fit to the change in absorbance values

corresponding to Pn concentrations above 1000 nM.

3.8.2 Optimization of Ancrod Concentration for Continuous Plasmin Generation in Plasma on a Fibrin Clot Assay

Various concentrations of Ancrod were added to NPP to initiate cleavage of fibrinogen and thus fibrin clot formation. Turbidity was monitored at 450 nm every 10 s to determine the optimal Ancrod concentration for clot formation. Increasing Ancrod concentrations resulted in a decreased time to clot formation, shown in Fig 26. An intermediate concentration of Ancrod, 0.6 U/ml, was chosen for the subsequent assays, with a clot formation time of approximately 300 s.
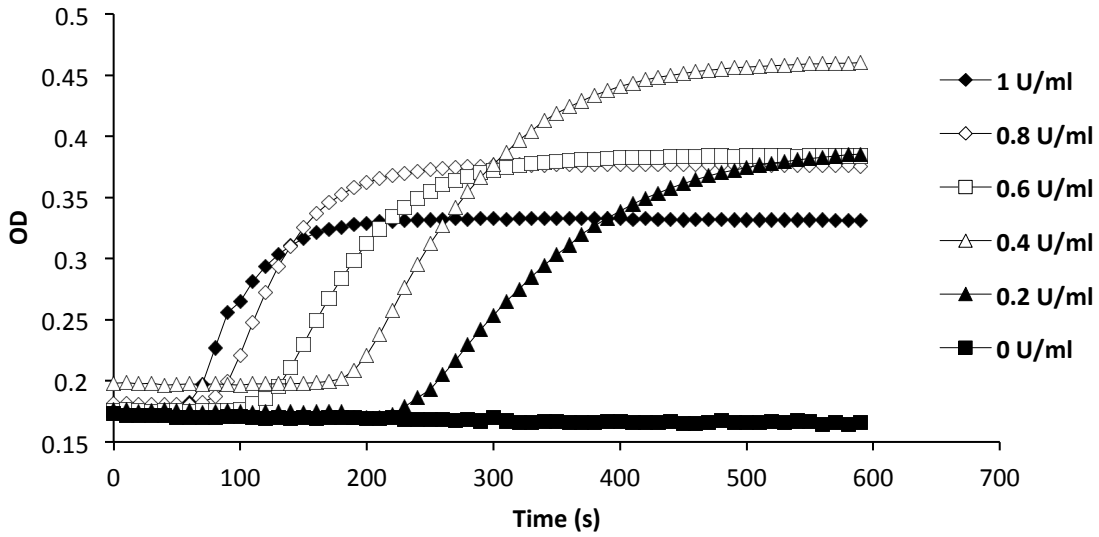
Figure 26. Optimizing Ancrod Concentration for Continuous Plasmin Generation in Plasma on Fibrin Clot Assay.

Various concentrations of Ancrod were added to 1/3 diluted NPP in TBS-T80 to initiate fibrin clot formation. Turbidity was measured every 10 s at 450 nm, for 2 hours at 37 °C. The first 600s of measurements are shown to highlight the timeframe of initial clot formation (n = 1).

3.8.3 Optimization of tPA Concentration for Continuous Plasmin Generation in Plasma on a Fibrin Clot Assay

Various concentrations of tPA were added to NPP in the presence of a fixed concentration of Ancrod (0.6 U/ml). Clot formation and lysis, and Pn activity (indicating Pn generation) were monitored at 450 and 405 nm every 10 s to determine optimal tPA concentration. At lower concentrations of tPA (0 and 0.125 nM) the clot did not lyse and minimal Pn was generated, within the experimental time frame. This is shown in Fig. 27 A in which absorbance at 405 nm (OD) did not increase significantly after clot formation shown in the corresponding graph in Fig. 27 B (plateau phase of absorbance). Turbidity also did not decrease for these conditions throughout the duration of the experiment, indicating absence of clot lysis (Fig. 27 B).

Increasing tPA concentration resulted in an increase in the rate of Pn generation and a decreased clot lysis time. In Fig. 27 B, 4.5 nM tPA resulted in a very fast clot lysis time (< 500 s) and very high corresponding Pn activity in Fig 28 A. A tPA concentration of 0.563 nM was selected in combination with 0.6 U/ml of Ancrod, as this resulted in a fast clot formation time (300 s) with a reasonable clot lysis time (~1600 s) that would enable the measurement of Pn formation on an unchanging clot surface (indicated by the plateau phase of turbidity) (Fig. 27 A and B).
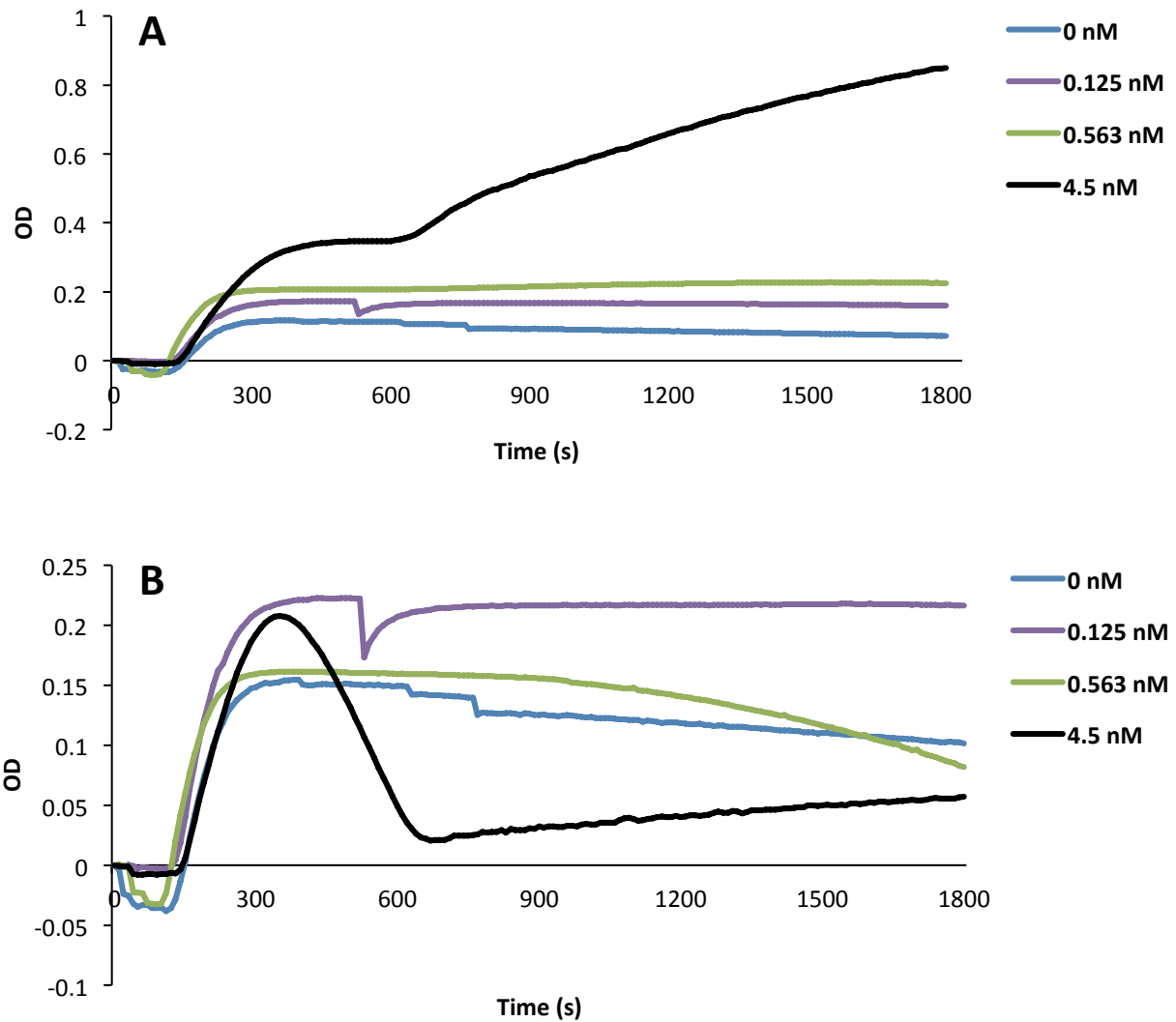
Figure 27. Optimizing tPA Concentration for Continuous Plasmin Generation in Plasma on Fibrin Clot Assay.

Various concentrations of tPA (final 0-4.5 nM) were added to 1/3 diluted NPP, 0.6 U/ml Ancrod, and 0.4 mM S2251 in TBS-T80 to initiate clot formation and Pn generation. Absorbance over 2 hours was measured at 405 and 450 nm. (A) Raw data of absorbance at 405 nm indicating combined Pn generation (thus subsequent S2251 cleavage) and turbidity from clot formation and lysis (n = 1). (B) Raw data of absorbance at 450 nm indicating clot formation and lysis only (n = 1).

3.9 Measuring Plasmin Generation Rates in Plasma on a Fibrin Clot

Ancrod and tPA were added to NPP ± UFH/ATH (0-2.1 U/ml) to initiate Pn generation. Pn activity was monitored over 2 hours with chromogenic substrate S2251. Initial rates of Pn generation were calculated as described in the Methods (Section 2.15.3). There were no differences in the initial rate of Pn generation in the presence and absence of UFH or ATH at all doses tested ($p = 0.840$) (Fig. 28).
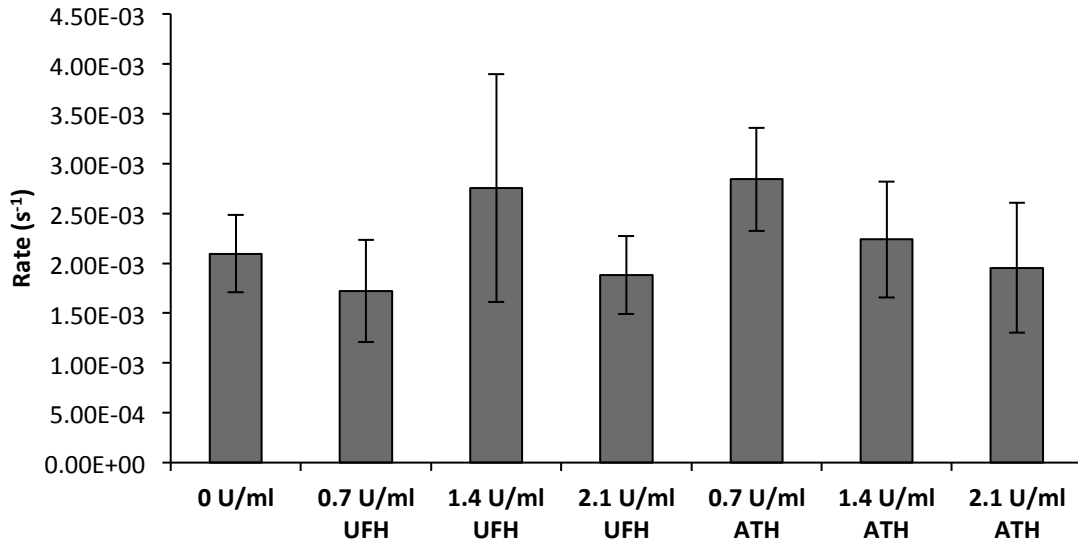
Figure 28. Initial Plasmin Generation Rates in Plasma on a Fibrin Clot, in the Presence of UFH or ATH.

Pn generation was initiated by the addition of tPA and Ancrod into 1/3 diluted NPP in TBS-T80. The change in absorbance over time, indicative of Pn generation was corrected for as described in Methods (Section 2.15.3) and plotted against time squared to obtain Pn generation rates. Initial rates of Pn generation ± 0.7-2.1 U/ml of UFH or ATH are shown in the bar graph above. Data represents mean of n = 5 ± SEM.

3.9.1 Clot Lysis by Plasmin Generated on a Fibrin Clot

Although there was no effect of the anticoagulants on initial Pn generation rates, it was of interest to observe whether the anticoagulants affected clot dissolution. Clot lysis times were determined from the previous Pn generation experiments in Section 3.9. UFH and ATH at 0.7-2.1 U/ml did not have an effect on clot lysis time when compared to the absence of anticoagulants ($p = 0.869$) (Fig. 29).
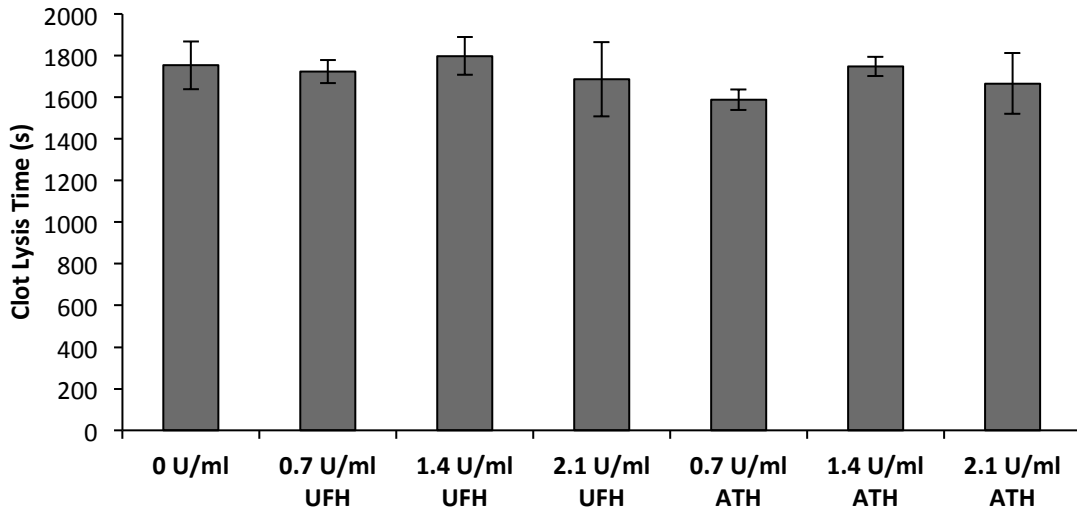
Figure 29. Clot Lysis Time of Fibrin Clot Lysed by Generated Plasmin.

Data from previous Pn generation experiments on fibrin clots (Section 3.9) were analyzed for

clot lysis times using the absorbance values at 450 nm (turbidity). Clot lysis time was defined as

the time in which turbidity had decreased to half its maximum absorbance value. The presence of

UFH or ATH at 0.7-2.1 U/ml were compared to the absence of anticoagulants (0 U/ml). Data

represents mean ± SEM (n = 5).

3.10 Clot lysis Time in the Presence of ATH

Due to the minimal effects of UFH and ATH at 0.7-2.1 U/ml on clot lysis times in previous experiments (Section 3.9.1), a high dose of ATH (10 U/ml) was added to PgdP that had been supplemented with various concentrations of Pg. Pn generation was initiated and clot lysis times were determined as previously described. Clot lysis times in the absence of ATH were approximately 1700 s, while in the presence of ATH, lysis times increased to > 2000 s (Fig. 30). In the presence of 10 U/ml of ATH, the Pg concentration did not affect clot lysis times (red bars) (p = 0.148). This independence of clot lysis time on Pg concentration was also seen with the absence of ATH (grey bars) (p = 0.660). When comparing the difference between ± 10 U/ml at each Pg concentration, there is a significant increase in clot lysis time in the presence of ATH at 800, 1600, 2000, and 3000 nM of Pg (p = 0.01, 0.026, 0.008, and 0.002, respectively).
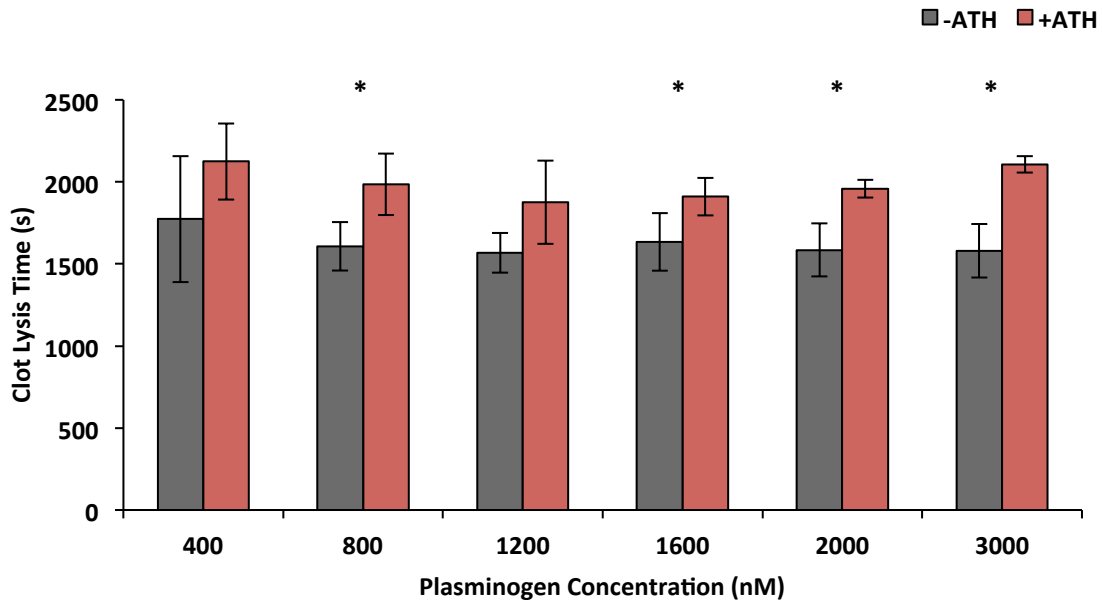
Figure 30. Clot Lysis Time in the Presence of 10 U/ml of ATH.

The clotlysis time in the absence of ATH (grey bars) at each Glu-Pg concentration was compared to the clot lysis time in the presence of 10 U/ml of ATH (red bars). Data shown is n = 5 ± SEM. * Represents a significant difference in clot lysis time between the presence and absence of ATH ($p < 0.05$).

3.11 Kinetics of Plasmin Generation in Plasma

To further investigate the mechanisms behind the observations in Section 3.9, in which low doses of UFH and ATH did not affect initial rate of Pn generation but increased the clot-lysis time at a high dose of ATH (Section 3.10), a Pn generation assay without a fibrin clot or Fib was developed.

3.11.1 Specific Activity of Plasmin with S2251 in Plasma

To convert change in absorbance (mOD/min), due to S2251 cleavage, to Pn concentration, various concentrations of Pn were incubated with S2251 in 1/3 diluted NPP in TSP. As seen in Fig. 31, there is a linear increase in change in absorbance with increasing Pn concentrations. A linear trendline was fit resulting in a model of $y = 0.134x-40.269$ and $R^2 = 0.956$. The specific activity (SA) of Pn was 0.134 mOD/min/nM (slope of linear equation).
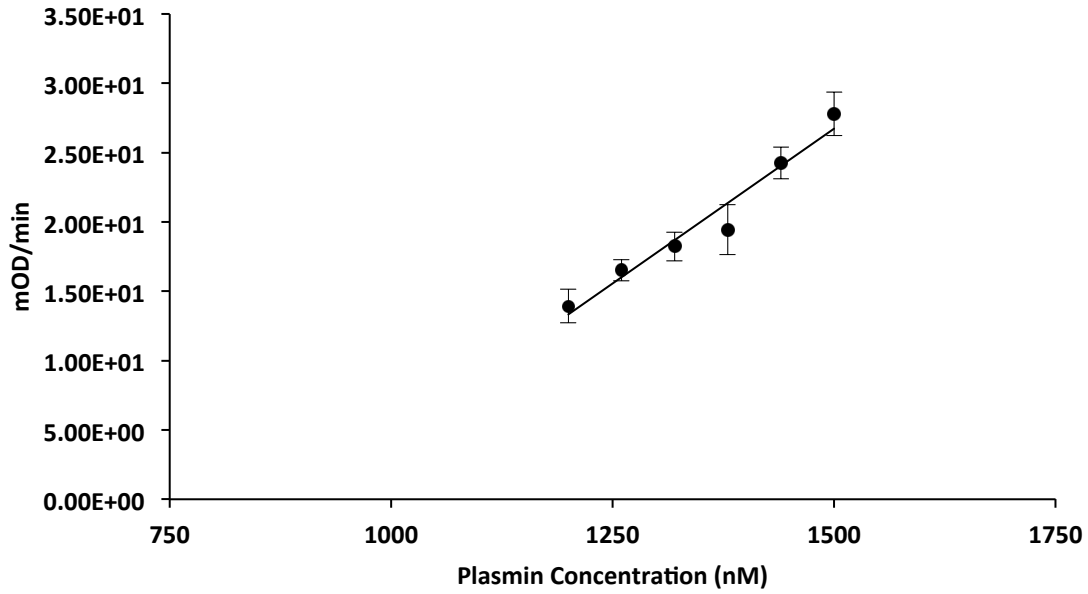
Figure 31. Specific Activity of Plasmin in Plasma.

Various concentrations of Pn (400-500 nM) were incubated with S2251 in 1/3 diluted NPP in

TSP. Change in absorbance over time (mOD/min) was monitored every 10 s for 1 hour at 405

nm (S2251 cleavage) and 450 nm (turbidity change). Change in absorbance (mOD/min) at 405

nm was plotted against corresponding Pn concentrations (adjusted for 100% plasma) and fitted to

linear trendline (solid).

3.11.2 Kinetics of Plasmin Generation in Plasma in the Presence of ATH or UFH

To observe the kinetics of the anticoagulant effect on Pn generation, a high dose of UFH or ATH (5 U/ml) was added to NPP prior to initiation of Pn generation with tPA. In the raw kinetic data, it can be seen that Pn activity is relatively similar in the beginning of the experiment (Fig. 32 A). However, as time increases, Pn activity decreases in the presence of UFH or ATH when compared to the absence of anticoagulants (Fig. 32 A). This is also evident in the first derivative, indicative of Pn generation rate (mOD/min versus min) (Fig. 32 B). The AUC was taken from the first derivative of each condition. UFH (2988.57 ± 166.63 nM•min) and ATH (2531.62 ± 160.09 nM•min) significantly decreased the Pn potential compared to the absence of anticoagulants (3794.82 ± 218.44 nM•min) ($p = 0.011$ and $p = 0.001$).
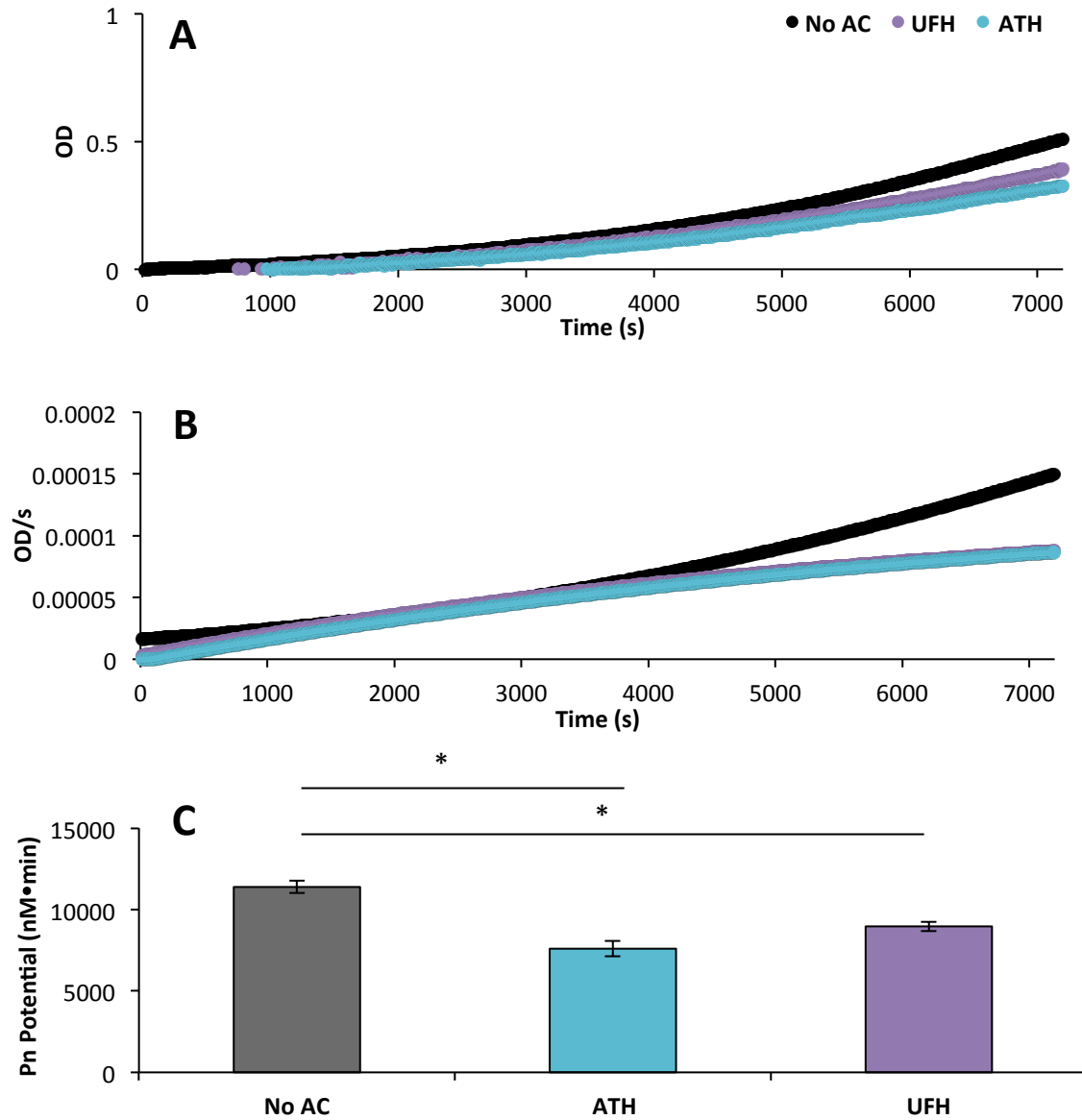
Figure 32. Plasmin Potential in the Presence of UFH or ATH.

Pn generation was initiated by adding tPA to S2251 and 1/3 diluted NPP ± 5 U/ml UFH/ATH.

Pn generation was monitored every 10 s for 2 hours at 405 nm and 450 nm. The first derivative

(B) was taken from the corresponding raw kinetic data (A). AUC (Pn concentration adjusted for

100% NPP) was calculated from the first derivatives and the presence of 5 U/ml of UFH/ATH

was compared to the absence of anticoagulants (C) (*$p < 0.01$).

4 Discussion

There have been extensive studies on the mechanism of action of ATH and comparison of its efficacy as an anticoagulant to commonly administered heparinoids. Despite its improved anticoagulant abilities compared to H, little is known about its interactions with other pathways of hemostasis, such as fibrinolysis. As past studies have suggested that H could have an effect on fibrinolysis, it was of interest to study the interactions of ATH and H with the components of the fibrinolytic pathway as they interact with coagulation factors through H mediated AT inhibition. Studies by Chander et al., provided insight on the interactions of ATH and mixtures of AT + UFH with Pn (the main serine protease of fibrinolysis). Although inhibition of Pn activity and generation was observed in the presence of both anticoagulants, these experiments were conducted in purified systems and hence only provide a partial understanding of anticoagulant effects on the fibrinolytic pathway. This study looks at the effect of ATH compared to UFH and LMWH on Pn generation in plasma. Although the experiments still study fibrinolysis in isolation (without coagulation) they involve the presence of natural Pn inhibitors, α_2-AP and α_2-M, and thus provide a better understanding of ATH's effect on fibrinolysis.

4.1 Comparison of Pn Generation Assay to Previously Published Methods

The experimental procedures of the first Pn generation assay in plasma, were originally adapted from previous studies by Parmar et al. (82). In comparison, the results of this current study were slightly different. The highest Pn concentration measured in this study was approximately 500 nM while Parmar et al. measured concentrations up to 800 nM. As well, the time frame of Pn generation was over 120 mins with subsampling every 20 mins, while this study was 60 mins in total (with 8 time points). It was observed, in this study, that Pn concentrations increased the most between 0-20 mins and leveled off from 60-120 mins.

84

Therefore to produce a curve in which Pn gradually increased, this study was conducted up to 60 mins with more closely timed subsampling increments. The steady increase in Pn concentration over time was considered an ideal curve as it would allow for the observation of any increase or decrease of the rate at which Pn was generated over time, in the presence of the anticoagulants studied.

The differences in this study compared to previous studies may be due to the type of soluble fibrin substitute used. Parmar et al. used commercially prepared Desafib. Desafib, also known as des-AA fibrin, is a solution of fibrin monomers that are naturally formed when IIa cleaves fibrinogen releasing fibrinopeptide A only (83,84). Desafib, used in experimental procedures, can be produced by snake venom such as reptilase (77,85). As Desafib was no longer commercially available, this study replaced it with cyanogen bromide digested fibrinogen fragments (Fib).

Studies by Liu et al., have compared the effects of Desafib and Fib mediated Pn generation by tPA and found that both promoted Pn generation greatly in comparison to fibrinogen (moderately promoted) and fragment E-2 (no stimulation) (76). Other studies looking at specific regions and sequences on fibrin that promote Pg activation, found that there are two D-regions that contain tPA and Pg binding sites: FCB-2 and FCB-5 (77,78,85). Both of these regions can also be found on Fib but are hidden in fibrinogen (86). Past studies looking at the kinetics of the activation of Pg by uPA and tPA (in the presence of fibrin) have also used Fib as a soluble fibrin substitute (87,88). As a result of these studies, Fib was deemed as a reasonable replacement for Desafib as a soluble fibrin substitute.

Although Fib was found to be an acceptable replacement for Desafib, the assay system required optimization as it was observed to be a very strong stimulator of Pn generation. In past

experiments in our lab, very low concentrations of Fib with the previously established amount of tPA (from Parmar et al.) produced a rapid increase in Pn at very early time points making it difficult to study the early stages of Pn generation. Therefore, adjustments to tPA and Fib concentrations were necessary to produce a curve with a quantifiable steady increase in Pn concentration over time. Once tPA and Fib concentrations were established, PA1-1 concentration was adjusted in order to effectively inhibit tPA mediated Pn generation, in subsamples, at various time points.

4.2 Inhibition of Plasmin Generation in Plasma in the Presence of Anticoagulants

The results from the Pn generation experiments were consistent with past *in* vitro studies in purified systems that indicated AT + UFH and ATH inhibit Pn and Pn generation (9). There was inhibition of Pn generation in the presence of UFH (at 0.7 U/ml) and ATH (at 0.7 and 2.1 U/ml) compared to the absence of anticoagulants (Fig. 13). This could be due to the interaction of the anticoagulants with tPA or AT inhibition of Pn, facilitated by H. The latter seems more plausible as previous experiments by Chander et al., indicated that UFH, ATH, and AT + UFH have no effect on tPA chromogenic activity (9). Therefore, it is likely that the decrease in Pn quantified, in the presence of the anticoagulants, was due to the inhibition of Pn by AT. This is congruent with the initial hypothesis (hypothesis 1 in Section 1.9) and is supported by past studies in which H enhanced AT inhibition of Pn through the conformational change mechanism (9,55,71-73).

It has been established that LMWH enhances AT inhibition of Xa and not IIa. This is due to its short chain length, which is only beneficial in facilitating a conformational change in AT (36). Therefore, it would have been expected that Pn inhibition in the presence of LMWH would be similar to UFH as they both have the same ability to inhibit Xa (89). However, contrary to

what was hypothesized (hypothesis 2 in Section 1.9), there was no significant inhibition of Pn generation by LMWH when compared to the presence and absence of UFH and ATH at all doses (Fig. 11, 12 and 13). The inability of LMWH to enhance AT inhibition of Pn suggests that AT inhibition of Pn may occur through a template-mediated effect. However, this is inconsistent with past studies that have suggested that H facilitates Pn inhibition by AT through the conformational change mechanism (9,72).

In addition, it was thought that ATH would inhibit Pn more than UFH (hypothesis 2 in Section 1.9) but there was no difference in Pn generation between ATH and UFH at any dose (Fig. 9 C and D). This suggests that although ATH is shown to be a more effective anticoagulant than UFH, they may have similar effects on fibrinolysis. There was also no clear dose dependent response due to any of the anticoagulants. Even with decreasing ATH doses from 0.1 U/ml to 0.001 U/ml, no dose dependent response was observed (Fig. 14). With the lower doses of ATH, an effect may not have been observed possibly due to small trial numbers (n = 3) or sensitivity of the assay to distinguish small differences. Another experiment that may be able to detect the slight differences would be a continuous assay measuring Pn generation (discussed in more detail below).

As Pn is generated, it is subsequently inhibited by α_2-AP and α_2-M (already present in plasma), which are faster inhibitors of Pn (53-55,71). AT may be the inferior competitor in comparison. Studies by Semeraro et al., have shown that Pn bound to AT (in the presence of H) was 4% in plasma compared to 16-21% when both α_2-AP and α_2-M were depleted from the plasma (55). Second order rate constants that have been reported for Pn inhibition by α_2-AP and α_2-M are 2.52×10^7 $M^{-1}s^{-1}$ and 3.67×10^5 $M^{-1}s^{-1}$, respectively (71). In comparison to 9.57×10^4 $M^{-1}s^{-1}$ for H catalyzed AT and 1.07×10^5 $M^{-1}s^{-1}$ for ATH (in the absence of fibrin), there is a

100-1000 times faster inhibition rate of Pn by α_2-AP (71). However, there is a smaller difference in rates when comparing the inhibition of Pn by H catalyzed AT or ATH with α_2-M. Therefore, at the initial doses tested (0.7-2.1 U/ml), Pn may already be quickly inhibited by α_2-AP but ATH and UFH may be able to compete with α_2-M for the remaining free Pn.

4.3 The Formation of Plasmin Bound α_2-Macroglobulin Complexes During Plasmin Generation

The plateau effect observed after 20 mins in the Pn generation graphs over time (Fig. 11) was due to the presence of α_2-M in plasma. The plateau suggested the depletion of Pg, no further Pn generation, and complete inhibition of all Pn produced. The residual Pn activity quantified with S2251, after 20 mins, was Pn bound to α_2-M, which still retains chromogenic activity (90). As seen in Fig. 17 A, Pn activity depicted in the two curves start similarly at 0 mins. At 10 mins, there is still free Pn in the system, indicated by the area between the two graphs. However, at 20 and 60 mins, the Pn amidolytic activity measured is mostly due to α_2-M bound Pn as both graphs converge to coinciding Pn concentrations. This pattern is also seen when quantifying for PAM complexes in the presence of UFH and ATH (not shown).

When comparing the AUC of PAM complexes, it was thought that ATH, UFH and LMWH would decrease the overall PAM complexes quantified (hypothesis 3 in Section 1.9). However, there was only a significant decrease observed at the highest doses of ATH tested (0.7 U/ml) compared to the absence of anticoagulants (Fig. 18). This may suggest, that although α_2-M and α_2-AP are faster inhibitors of Pn, ATH could compete with α_2-M at higher doses. This supports the Pn inhibition rate comparisons between α_2-M, α_2-AP, and AT as mentioned.

4.4 Quantification of Plasmin-α_2-AP During Plasmin Generation in Plasma

The Technozym PAP Complex ELISA was used to quantify PAP complexes in Pn generation subsamples. It had minimal cross reactivity with purified PAM, Pn, UFH, ATH, and NPP at concentrations that would be found in the Pn generation subsamples (Fig. 20). Thus, it was deemed specific for PAP complexes and Pn generation subsamples were tested. The results obtained from the same conditions on different days displayed minimal variability. The ELISA was able to illustrate the formation of PAP complexes during the Pn generation experiments (Fig. 21). There were minimal PAP complexes in subsamples that were taken right after initiation of Pn generation. The maximum amounts of PAP complexes were formed at 20 mins. The highest concentration quantified was approximately 1600 nM or 1.6 μM, which is slightly higher than the 1 μM average of α_2-AP found in plasma (54). It was hypothesized that ATH, UFH, and LMWH would all decrease PAP formation (hypothesis 3 in Section 1.9) but there were no differences in the total PAP complexes formed in the presence or absence of UFH and ATH. This was now expected as close review of the literature shows that the rates of Pn inhibition by α_2-AP is much faster than UFH + AT and ATH (71).

4.5 Plasminogen Consumption During Plasmin Generation

To confirm that anticoagulants had limited effects on tPA activity, the consumption of Pg during Pn generation was monitored. Prior to measuring Pn generation subsamples, it was noted that UFH did not interfere with Pg quantification in NPP. The kit did not detect any Pg in PgdP and it did not cross-react with purified Pn (Fig. 23 B and C). This indicated that the kit was specific for Pg. There was a slight decrease in Pg concentrations in NPP when ATH was added. Only one trial was conducted of these controls and therefore the slight decrease in Pg from the presence of ATH could be due to experimental variability.

Pg was quantified in Pn generation subsamples by ELISA. The starting levels of Pg were lower than expected, at approximately 600 nM, while according to the literature, average plasma levels are 1.5-2 μM (53,54). It was initially thought that this difference was due to the possible limitations of the Pn generation assay. More specifically, there was a delay between the initiation of Pn generation and taking the first subsample (corresponding to 0 s) of approximately 10-20 s. Within this short time frame, possibly the conversion rate of Pg to Pn by tPA was so quick that some Pg may have already been converted before subsampling. However, low initial Pn and PAP concentrations (Fig. 11 and Fig. 21) do not support this theory. Hence, another cause could have been an over dilution of samples when tested in the ELISA, although samples were diluted based on the kit instructions.

The largest decrease in Pg was from 0 to 10 mins (from approximately 600 nM to 200 nM) (Fig. 24). There were no differences in Pg consumption observed between the two doses of UFH or ATH compared to the absence of these anticoagulants. This suggests that the anticoagulants had no effect on tPA activity as any changes in Pg consumption would indicate interference with the enzyme that cleaves it to form Pn. This agrees with previous studies that found UFH + AT and ATH had no effect on tPA chromogenic activity (9). Furthermore, the plateau between 20 and 60 mins, in which no further Pg is consumed, supports the evidence from Fig. 11 that Pn generation is completed at about 20 mins in Fig. 11.

4.6 Anticoagulant Effect on Rates of Pn Generation on a Fibrin Clot in Plasma

The Pn generation assays in Section 3.4 had some possible limitations. One concern was S2251 depletion, which would result in inaccurate measures of Pn concentrations at each timed subsample. Although previous tests showed that a 20 min incubation period of subsamples with S2251 did not result in its depletion (data not shown) it was not possible to verify that this did

not occur during the actual Pn generation experiments. As well, because the experiments were monitored via subsampling, there were no observations available for periods in between the time points. In efforts to confirm that this assay was accurate in monitoring differences in Pn generation over time (in the presence and absence of anticoagulants) a continuous assay was performed. This assay would allow for uninterrupted measurement of Pn activity during Pn generation. The Pn generation assay on fibrin clots (Methods Section 2.11) had been adapted from previous studies by Chander et al., measuring Pn generation kinetics in purified systems (9). The fibrin clot would replace the Fib that was used in the discontinuous Pn generation experiments in plasma. From all previous experiments it seems apparent that any effect the anticoagulants had on the rate of Pn generation was due to the inhibition of Pn activity. Any inhibitory effect was not from interactions with tPA as the Pg ELISA experiments showed no difference in rate of Pg consumption rate in the presence of the anticoagulants (Fig. 24).

The Pn generation experiments, on fibrin clots, were conducted in the presence of 0-2.1 U/ml of UFH or ATH (the same doses as Section 3.4). There were no significant differences in the initial Pn generation rates between all doses of both anticoagulants compared to the absence of these anticoagulants (Fig. 28). These results were different from the results of the previous discontinuous assay seen in the Section 3.4 (Fig. 12). However, only initial rates from the first 10-15% of Pn generation were measured. In these initial stages of Pn generation, there may be no difference due to the presence of α_2-AP and some α_2-M that are inhibiting the Pn as it is generated. It was mentioned that α_2-AP has a much higher rate of Pn inhibition than AT + UFH and ATH and the PAP ELISA experiments show that UFH and ATH have no effect on PAP complex formation. Thus, the presence of α_2-AP could possibly mask any small amount of Pn initially inhibited by ATH and UFH facilitated AT, in these continuous experiments.

In addition, this may explain the discrepancies between the results found in the Pn generation rate experiments by Chander et al. and that of this study. Chander et al. measured up to a 38-fold decrease in initial Pn generation rates in the presence of ATH compared to UFH + AT at similar concentrations (9). However, such assays did not include the presence of α_2-AP and α_2-M and therefore it can be concluded that in the absence of Pn's natural inhibitors, UFH and ATH are capable of inhibiting Pn activity greatly. However, with α_2-AP and α_2-M present *in vivo* the effect of UFH and ATH on Pn activity may be minimal.

4.7 Anticoagulant Effect on Clot-Lysis Time

To further investigate whether any possible inhibition of Pn by the anticoagulants affected clot degradation, clot-lysis time was determined from Pn generation assays on fibrin clots (in plasma) (Fig. 29) and in PgdP with various concentrations of added Glu-Pg (Fig. 30). The addition of 0.7-2.1 U/ml of UFH or ATH did not affect clot-lysis times during Pn generation on fibrin clots (Fig. 29). Interestingly, the addition of a very high dose of ATH ($> 10 \times$ higher than therapeautic doses of UFH) into PgdP (with various Glu-Pg concentrations), resulted in a significant increase in clot-lysis time at 800, 1600, 2000, and 3000 nM of Glu-Pg. Due to the fact that clot formation was not from IIa (but from Ancrod), the increase in clot-lysis time, was solely due to Pn inhibition and not inhibition of coagulation. It is suggested that once α_2-AP is depleted (as UFH or ATH had no effect on PAP complexes in Fig. 21) the high dose of ATH (10 U/ml) could compete with α_2-M to inhibit residual Pn. This would lead to a decreased amount of Pn binding to the fibrin, clot and subsequently decreased fibrin cleavage. This supports why 0.7 U/ml of ATH was able to decrease the amount of PAM complexes formed in previous Pn generation experiments. However, the increased clot lysis time due to Pn inhibition with high doses of ATH may not elicit similar outcomes *in vivo,* with coagulation and anticoagulation

coexisting with fibrinolysis. This is suggested in a past study by Klement et al., showing that ATH reduced microemboli formation in a cardiopulmonary bypass pig model, in a dose dependent manner indicating that even at high doses of ATH, *in vivo*, fibrinolysis was not inhibited (50).

4.8 Mechanism Behind Increased Clot-lysis Time in the Presence of High Dose of ATH

To provide insight as to the mechanisms of how high doses of ATH (10 U/ml) affected clot-lysis times, a continuous Pn generation experiment in plasma without fibrin clots or Fib was performed in the presence of 5 U/ml of UFH or ATH (Methods Section 2.12, Results Section 3.11.2). Initially, very high doses (10 U/ml) were tested, however, it was noted that precipitation was forming. This was possibly due to S2251 interaction with H chains. Thus, the doses of anticoagulants tested in these experiments were decreased to 5 U/ml, which was the highest dose that did not result in visible precipitate forming prior to initiating Pn generation experiments. Despite no precipitation forming, whether S2251 interaction with H interfered with the overall mechanisms studied is uncertain. In addition, clot lysis experiments also used 10 U/ml of ATH, as mentioned above. However, as the assays were based on turbidity, it could not be ruled out that precipitate did not form. These are possible limitations to this study.

As seen in Fig. 32 B, the first derivatives, indicative of the rate of Pn generation, show that Pn generation rates are similar in the first half (approximately 3000 s) of the experiment in the presence or absence of UFH and ATH. This may explain the lack of differences in the initial rates of Pn generation on fibrin clots, in plasma with UFH or ATH (0.7-2.1 U/ml) (Fig. 28).

After approximately 3000 s, the rates of Pn generation in the presence of UFH and ATH start to decrease, while in the absence of anticoagulants, Pn generation continues to increase. This time frame may indicate the depletion of all the free α_2-AP from the plasma (due to Pn

binding) and successive Pn generated is competed for by α_2-M, UFH bound AT, or ATH. This supports the past experiments in which 0.7 U/ml ATH was seen to decrease PAM complex formation during Pn generation. The decrease in Pn generation rate seen after 3000 s resulted in a lowered Pn potential in the presence of UFH and ATH when compared to the absence of anticoagulants (Fig. 32 C). This decreased Pn potential, is consistent with the increased clot lysis times seen with a high dose of ATH, discussed in Section 4.7.

The results of this assay do not explain the significant decrease in AUC observed in Fig. 12 and Fig. 13 in the presence of 0.7 U/ml and 2.1 U/ml of ATH and 0.7 U/ml of UFH when compared to the absence of these anticoagulants. However, the two assay types do have their differences. The continuous Pn generation assay in plasma (Fig. 32) did not include fibrin clots or soluble fibrin substitutes, therefore a slower rate of Pn generation (and a lower amount of Pn) would occur compared to the assays conducted in Section 3.4. As a result, there were no effects seen when lower doses of UFH or ATH were added (data not shown) as lower concentrations of Pn were produced over time and there may not have been enough Pn to show a decrease in activity caused by α_2-AP, α_2-M, UFH, and ATH inhibition combined. Thus only when a higher dose was tested, could UFH or ATH overcome the presence of α_2-AP and α_2-M and exhibit a decrease in Pn activity nearing the end of the experiments (Fig. 32 B).

Another limitation of the continuous assays (on a fibrin clot or without) is that S2251 is present while Pn generation and inhibition occurs. It has been previously observed (in our lab) that S2251 may interact with H chains. This could also explain the precipitation effect at high doses of UFH and ATH discussed in Section 4.8. The effect of this is unclear, however it can be postulated that the sequestering of S2251 on H chains could interfere with H interactions with AT or interactions with Pn. Thus, in such assays in which kinetic rates are measured, in the

presence of heparinoids, careful considerations must be made when extrapolating conclusions from the data obtained.

5 Future Directions

Gathering from this work, UFH facilitated AT and ATH can inhibit Pn activity. However, in the presence of its natural inhibitors and during clot degradation this effect may be minimal. This study solely isolates for fibrinolysis and does not include the interactions between UFH, ATH and coagulation. Hence, future studies should be directed at this interaction. For example, it has been established that the generation of IIa and its relative concentrations during clot formation affects clot structure and stability. This in turn can affect the rate of fibrinolysis (91). In this study, the fibrin clots produced were as a result of Ancrod and thus these results may change, *in vivo,* depending on local IIa levels.

In the presence of thrombomodulin (TM), IIa activates thrombin-activatable fibrinolysis inhibitor (TAFI), which is involved in the cleavage of carboxy-terminal lysine residues on fibrin (92). This eliminates Pg binding sites and therefore inhibits further Pn generation (92). The presence of UFH and ATH under these conditions would decrease the amount of IIa and prevent TAFI activation. This would lead to the continuation of fibrinolysis and clot dissolution. Although in this study UFH and ATH inhibited Pn activity and ATH increased clot lysis time (at higher than therapeutic doses), this effect may not be observed *in vivo.* This is due to the simultaneous occurrence of coagulation and the interaction of these anticoagulants with IIa and other coagulation factors resulting in decreased interactions with overall fibrinolysis.

Furthermore, ATH has been reported to inhibit IIa bound TM (93). This is notable as not only does TM enhance IIa activation of TAFI but it also enhances IIa activation of Protein C (92). Protein C is an anticoagulant that inactivates Factors Va and VIIIa, which stops further IIa

generation (94). The decrease in IIa levels would also decrease TAFI activation and once again, will allow fibrinolysis to continue. Future studies on the anticoagulants effect on IIa generation and subsequently TAFI activation could further investigate this.

6 Summary

Thus far, it has been observed that in purified systems, UFH and ATH can both inhibit Pn activity/generation rates and this current study supports this (9). In the quantification of Pg consumption, it was inferred that any effect on Pn generation was not due to anticoagulant effects on tPA. The inhibitory effect by anticoagulants seen in Pn generation experiments could be minimal *in vivo*, as in comparison to α_2-AP and possibly α_2-M, UFH and ATH are the slower inhibitors of Pn. This is supported by the lack of difference in clot lysis times in the absence and presence of these anticoagulants at similar doses (0.7-2.1 U/ml). It was only at a very high dose of ATH (10 U/ml, $> 10 \times$ therapeutic dose of UFH) that increased clot-lysis times were observed, suggesting that the inhibitory effect on Pn may not be substantial enough to affect overall fibrinolysis *in vivo*. As well, the quantification of PAP complexes demonstrated that the anticoagulants had no effect on the formation of this enzyme-inhibitor complex and thus α_2-AP activity. The quantification of PAM complexes implied that ATH might be able to compete with α_2-M but only at very high doses. These observations provide a better understanding of the interactions of ATH compared to UFH and LMWH with the components of fibrinolysis under more physiological conditions. Upon evaluation of this study, it can be inferred that ATH may not have a significant inhibitory effect on fibrinolysis and therefore will primarily contribute to regulating coagulation and ultimately be an effective agent in reducing thrombosis *in vivo* through that mechanism.

7 References

(1) Murray R, Rodwell V, Bender D et al. Hemostasis and Thrombosis. Harper's Illustrate Biochemistry. Toronto: McGraw Hill Professional, 2009.

(2) Boon GD. An overview of hemostasis. *Toxicol Pathol.* 1993;21(2):170-179.

(3) Wolberg AS, Aleman MM, Leiderman K, Machlus KR. Procoagulant activity in hemostasis and thrombosis: Virchow's triad revisited. *Anesth Analg.* 2012;114(2):275-285.

(4) Desai UR. New antithrombin-based anticoagulants. *Med Res Rev.* 2004;24(2):151-181.

(5) Berry LR, Becker DL, Chan AK. Inhibition of fibrin-bound thrombin by a covalent antithrombin-heparin complex. *J Biochem.* 2002;132(2):167-176.

(6) Chan AK, Berry L, Klement P et al. A novel antithrombin-heparin covalent complex: antithrombotic and bleeding studies in rabbits. *Blood Coagul Fibrinolysis.* 1998;9(7):587-595.

(7) Mewhort-Buist TA, Junop M, Berry LR et al. Structural effects of a covalent linkage between antithrombin and heparin: covalent N-terminus attachment of heparin enhances the maintenance of antithrombin's activated state. *J Biochem.* 2006;140(2):175-184.

(8) Patel S, Berry LR, Chan AK. Analysis of inhibition rate enhancement by covalent linkage of antithrombin to heparin as a potential predictor of reaction mechanism. *J Biochem.* 2007;141(1):25-35.

(9) Chander A, Atkinson HM, Stevic I et al. Interactions of heparin and a covalently-linked antithrombin-heparin complex with components of the fibrinolytic system. *Thromb Haemost.* 2013;110(6):1180-1188.

(10) Murray R, Rodwell V, Bender D et al. Hemostasis and Thrombosis. Harper's Illustrate Biochemistry. Toronto: McGraw Hill Professional, 2009.

(11) Smith SA. The cell-based model of coagulation. *J Vet Emerg Crit Care (San Antonio).* 2009;19(1):3-10.

(12) Hoffman M, Monroe DM, III. A cell-based model of hemostasis. *Thromb Haemost.* 2001;85(6):958-965.

(13) Olson ST, Frances-Chmura AM, Swanson R et al. Effect of individual carbohydrate chains of recombinant antithrombin on heparin affinity and on the generation of glycoforms differing in heparin affinity. *Arch Biochem Biophys.* 1997;341(2):212-221.

(14) Wolberg AS, Campbell RA. Thrombin generation, fibrin clot formation and hemostasis. *Transfus Apher Sci.* 2008;38(1):15-23.

(15) Sidelmann JJ, Gram J, Jespersen J, Kluft C. Fibrin clot formation and lysis: basic mechanisms. *Semin Thromb Hemost.* 2000;26(6):605-618.

(16) Eyre L, Gamlin F. Haemostasis, blood platelets and coagulation. 2010;11(6):244-246.

(17) De Caterina R, Husted S, Wallentin L et al. General mechanisms of coagulation and targets of anticoagulants (Section I). Position Paper of the ESC Working Group on Thrombosis--Task Force on Anticoagulants in Heart Disease. 2013;109(4):569-579.

(18) Becker BF, Heindl B, Kupatt C, Zahler S. Endothelial function and hemostasis. 2000;89(3):160-167.

(19) de Groot PG, Urbanus RT, Roest M. Platelet interaction with the vessel wall. 2012;(210):87-110.

(20) Lankhof H, van Hoeij M, Schiphorst ME et al. A3 domain is essential for interaction of von Willebrand factor with collagen type III. 1996;75(6):950-958.

(21) Leger AJ, Covic L, Kuliopulos A. Protease-activated receptors in cardiovascular diseases. 2006;114(10):1070-1077.

(22) Camire RM, Pollak ES, Kaushansky K, Tracy PB. Secretable human platelet-derived factor V originates from the plasma pool. 1998;92(9):3035-3041.

(23) Tanaka KA, Key NS, Levy JH. Blood coagulation: hemostasis and thrombin regulation. 2009;108(5):1433-1446.

(24) Lentz BR. Exposure of platelet membrane phosphatidylserine regulates blood coagulation. 2003;42(5):423-438.

(25) Baglia FA, Shrimpton CN, LÃ³pez JA, Walsh PN. The glycoprotein Ib-IX-V complex mediates localization of factor XI to lipid rafts on the platelet membrane. 2003;278(24):21744-21750.

(26) Bradford HN, Pixley RA, Colman RW. Human factor XII binding to the glycoprotein Ib-IX-V complex inhibits thrombin-induced platelet aggregation. 2000;275(30):22756-22763.

(27) Heemskerk JW, Mattheij NJ, Cosemans JM. Platelet-based coagulation: different populations, different functions. 2013;11(1):2-16.

(28) Lahav J, Tvito A, Bagoly Z et al. Factor XIII improves platelet adhesion to fibrinogen by protein disulfide isomerase-mediated activity. 2013;131(4):338-341.

(29) Magwenzi SG, Ajjan RA, Standeven KF et al. FactorÂ XIII supports platelet activation and enhances thrombus formation by matrix proteins under flow conditions. 2011;9(4):820-833.

(30) Quinsey NS, Greedy AL, Bottomley SP et al. Antithrombin: in control of coagulation. *Int J Biochem Cell Biol.* 2004;36(3):386-389.

(31) McCoy AJ, Pei XY, Skinner R et al. Structure of beta-antithrombin and the effect of glycosylation on antithrombin's heparin affinity and activity. *J Mol Biol.* 2003;326(3):823-833.

(32) Picard V, Ersdal-Badju E, Bock SC. Partial glycosylation of antithrombin III asparagine-135 is caused by the serine in the third position of its N-glycosylation consensus sequence and is responsible for production of the beta-antithrombin III isoform with enhanced heparin affinity. *Biochemistry.* 1995;34(26):8433-8440.

(33) Casu B, Lindahl U. Structure and biological interactions of heparin and heparan sulfate. *Adv Carbohydr Chem Biochem.* 2001;57:159-206.

(34) Hirsh J, Anand SS, Halperin JL, Fuster V. Guide to anticoagulant therapy: Heparin : a statement for healthcare professionals from the American Heart Association. *Circulation.* 2001;103(24):2994-3018.

(35) Olson ST, Bjork I, Sheffer R et al. Role of the antithrombin-binding pentasaccharide in heparin acceleration of antithrombin-proteinase reactions. Resolution of the antithrombin conformational change contribution to heparin rate enhancement. *J Biol Chem.* 1992;267(18):12528-12538.

(36) Hirsh J, Warkentin TE, Shaughnessy SG et al. Heparin and low-molecular-weight heparin: mechanisms of action, pharmacokinetics, dosing, monitoring, efficacy, and safety. *Chest.* 2001;119(1 Suppl):64S-94S.

(37) Chan A, Berry L, O'Brodovich H et al. Covalent antithrombin-heparin complexes with high anticoagulant activity. Intravenous, subcutaneous, and intratracheal administration. *J Biol Chem.* 1997;272(35):22111-22117.

(38) Chan AK, Paredes N, Thong B et al. Binding of heparin to plasma proteins and endothelial surfaces is inhibited by covalent linkage to antithrombin. *Thromb Haemost.* 2004;91(5):1009-1018.

(39) Patel S, Berry LR, Chan AK. Covalent antithrombin-heparin complexes. *Thromb Res.* 2007;120(2):151-160.

(40) Smith LJ, Mewhort-Buist TA, Berry LR, Chan AK. An antithrombin-heparin complex increases the anticoagulant activity of fibrin clots. *Res Lett Biochem.* 2008;2008:639829.

(41) Chan AK, Berry LR, Paredes N, Parmar N. Isoform composition of antithrombin in a covalent antithrombin-heparin complex. *Biochem Biophys Res Commun.* 2003;309(4):986-991.

(42) Weitz JI, Hudoba M, Massel D et al. Clot-bound thrombin is protected from inhibition by heparin-antithrombin III but is susceptible to inactivation by antithrombin III-independent inhibitors. *J Clin Invest.* 1990;86(2):385-391.

(43) Brufatto N, Ward A, Nesheim ME. Factor Xa is highly protected from antithrombin-fondaparinux and antithrombin-enoxaparin when incorporated into the prothrombinase complex. *J Thromb Haemost.* 2003;1(6):1258-1263.

(44) Chan AK, Rak J, Berry L et al. Antithrombin-heparin covalent complex: a possible alternative to heparin for arterial thrombosis prevention. *Circulation.* 2002;106(2):261-265.

(45) Weitz JI, Leslie B, Hudoba M. Thrombin binds to soluble fibrin degradation products where it is protected from inhibition by heparin-antithrombin but susceptible to inactivation by antithrombin-independent inhibitors. *Circulation.* 1998;97(6):544-552.

(46) Atkinson HM, Mewhort-Buist TA, Berry LR, Chan AK. Anticoagulant mechanisms of covalent antithrombin-heparin investigated by thrombelastography. Comparison with unfractionated heparin and low-molecular-weight heparin. *Thromb Haemost.* 2009;102(1):62-68.

(47) Stevic I, Chan HH, Chander A et al. Covalently linking heparin to antithrombin enhances prothrombinase inhibition on activated platelets. *Thromb Haemost.* 2013;109(6):1016-1024.

(48) Stevic I, Berry LR, Chan AK. Mechanism of inhibition of the prothrombinase complex by a covalent antithrombin-heparin complex. *J Biochem.* 2012;152(2):139-148.

(49) Stevic I, Chan HH, Berry LR et al. Inhibition of the prothrombinase complex on red blood cells by heparin and covalent antithrombin-heparin complex. *J Biochem.* 2013;153(1):103-110.

(50) Klement P, Berry LR, Liao P et al. Antithrombin-heparin covalent complex reduces microemboli during cardiopulmonary bypass in a pig model. *Blood.* 2010;116(25):5716-5723.

(51) Medved L, Nieuwenhuizen W. Molecular mechanisms of initiation of fibrinolysis by fibrin. *Thromb Haemost.* 2003;89(3):409-419.

(52) Cesarman-Maus G, Hajjar KA. Molecular mechanisms of fibrinolysis. *British journal of haematology.* 2005;129(3):307-321.

(53) Lijnen HR. Elements of the fibrinolytic system. *Ann N Y Acad Sci.* 2001;936:226-236.

(54) Schaller J, Gerber SS. The plasmin-antiplasmin system: structural and functional aspects. *Cell Mol Life Sci.* 2011;68(5):785-801.

(55) Semeraro N, Colucci M, Telesforo P, Collen D. The inhibition of plasmin by antithrombin-heparin complex. I. In human plasma in vitro. *Br J Haematol.* 1978;39(1):91-99.

(56) Collen D, Semeraro N, Telesforo P, Verstraete M. Inhibition of plasmin by antithrombin-heparin complex. II. During thrombolytic therapy in man. *Br J Haematol.* 1978;39(1):101-110.

(57) Edelberg JM, Pizzo SV. Kinetic analysis of the effects of heparin and lipoproteins on tissue plasminogen activator mediated plasminogen activation. *Biochemistry.* 1990;29(25):5906-5911.

(58) Edelberg JM, Conrad HE, Pizzo SV. Heparin oligosaccharides enhance tissue-type plasminogen activator: a correlation between oligosaccharide length and stimulation of plasminogen activation. *Biochemistry.* 1991;30(45):10999-11003.

(59) Liang JF, Li Y, Yang VC. The potential mechanism for the effect of heparin on tissue plasminogen activator-mediated plasminogen activation. *Thromb Res.* 2000;97(5):349-358.

(60) Andrade-Gordon P, Strickland S. Anticoagulant low molecular weight heparin does not enhance the activation of plasminogen by tissue plasminogen activator. *J Biol Chem.* 1989;264(26):15177-15181.

(61) Andrade-Gordon P, Strickland S. Fractionation of heparin by chromatography on a tissue plasminogen activator-Sepharose column. *Proc Natl Acad Sci U S A.* 1990;87(5):1865-1869.

(62) Fears R. Kinetic studies on the effect of heparin and fibrin on plasminogen activators. *Biochem J.* 1988;249(1):77-81.

(63) Nishino T, Yamauchi T, Horie M et al. Effects of a fucoidan on the activation of plasminogen by u-PA and t-PA. *Thromb Res.* 2000;99(6):623-634.

(64) Paques EP, Stohr HA, Heimburger N. Study on the mechanism of action of heparin and related substances on the fibrinolytic system: relationship between plasminogen activators and heparin. *Thromb Res.* 1986;42(6):797-807.

(65) Vinazzer H. [Investigations of the fibrinolytic effect of heparin]. *Wien Z Inn Med.* 1951;32(4):167-173.

(66) Andrade-Gordon P, Strickland S. Interaction of heparin with plasminogen activators and plasminogen: effects on the activation of plasminogen. *Biochemistry.* 1986;25(14):4033-4040.

(67) Vinazzer H, Stemberger A, Haas S, Blumel G. Influence of heparin; of different heparin fractions and of a low molecular weight heparin-like substance on the mechanism of fibrinolysis. *Thromb Res.* 1982;27(3):341-352.

(68)   Bell J, Duhon S, Doctor VM. The effect of fucoidan, heparin and cyanogen bromide-fibrinogen on the activation of human glutamic-plasminogen by tissue plasminogen activator. *Blood Coagul Fibrinolysis.* 2003;14(3):229-234.

(69)   Young TN, Edelberg JM, Stack S, Pizzo SV. Ionic modulation of the effects of heparin on plasminogen activation by tissue plasminogen activator: the effects of ionic strength, divalent cations, and chloride. *Arch Biochem Biophys.* 1992;296(2):530-538.

(70)   Rijken DC, de Munk GA, Jie AF. Interaction of plasminogen activators and plasminogen with heparin: effect of ionic strength. *Thromb Haemost.* 1993;70(5):867-872.

(71)   Anonick PK, Wolf B, Gonias SL. Regulation of plasmin, miniplasmin, and streptokinase-plasmin complex by alpha 2-antiplasmin, alpha 2-macroglobulin, and antithrombin III in the presence of heparin. *Thromb Res.* 1990;59(3):449-462.

(72)   Jordan RE, Oosta GM, Gardner WT, Rosenberg RD. The kinetics of hemostatic enzyme-antithrombin interactions in the presence of low molecular weight heparin. *J Biol Chem.* 1980;255(21):10081-10090.

(73)   Highsmith RF, Rosenberg RD. The inhibition of human plasmin by human antithrombin-heparin cofactor. *J Biol Chem.* 1974;249(14):4335-4338.

(74)   Teger-Nilsson AC, Friberger P, Gyzander E. Determination of a new rapid plasmin inhibitor in human blood by means of a plasmin specific tripeptide substrate. *Scand J Clin Lab Invest.* 1977;37(5):403-409.

(75)   Weitz JI, Kuint J, Leslie B, Hirsh J. Standard and low molecular weight heparin have no effect on tissue plasminogen activator induced plasma clot lysis or fibrinogenolysis. *Thromb Haemost.* 1991;65(5):541-544.

(76)   Liu JN, Gurewich V. A comparative study of the promotion of tissue plasminogen activator and pro-urokinase-induced plasminogen activation by fragments D and E-2 of fibrin. *J Clin Invest.* 1991;88(6):2012-2017.

(77)   Nieuwenhuizen W, Vermond A, Voskuilen M et al. Identification of a site in fibrin(ogen) which is involved in the acceleration of plasminogen activation by tissue-type plasminogen activator. *Biochim Biophys Acta.* 1983;748(1):86-92.

(78)   Nieuwenhuizen W, Verheijen JH, Vermond A, Chang GT. Plasminogen activation by tissue activator is accelerated in the presence of fibrin(ogen) cyanogen bromide fragment FCB-2. *Biochim Biophys Acta.* 1983;755(3):531-533.

(79)   Nieuwenhuizen W, Keyser J. Species specificity in the acceleration of tissue-type plasminogen activator-mediated activation of plasminogens, by fibrinogen cyanogen bromide fragments. *Thromb Res.* 1985;38(6):663-670.

(80) Nieuwenhuizen W, Voskuilen M, Vermond A et al. The influence of fibrin(ogen) fragments on the kinetic parameters of the tissue-type plasminogen-activator-mediated activation of different forms of plasminogen. *Eur J Biochem.* 1988;174(1):163-169.

(81) Kim PY, Tieu LD, Stafford AR et al. A high affinity interaction of plasminogen with fibrin is not essential for efficient activation by tissue-type plasminogen activator. *Journal of Biological Chemistry.* 2012;287(7):4652-4661.

(82) Parmar N, Mitchell LG, Berry LR et al. The influence of age on in vitro plasmin generation in the presence of fibrin monomer. *Acta Haematol.* 2006;115(3-4):141-151.

(83) Lougovskoi EV, Gogolinskaya GK. Preparation of fibrin des-AA by thrombin. *Ukr Biokhim Zh.* 1999;71(4):107-108.

(84) Brosstad F, Godal HC. Incomplete transformation of plasma fibrinogen to fibrin. Fibrinogen content and streptokinase-induced intra-clot lysis susceptibility of des-AA or des-AABB fibrin clots formed at varying fibrinogen/fibrin ratios. *Thromb Res.* 1979;14(2-3):507-512.

(85) Verheijen JH, Nieuwenhuizen W, Wijngaards G. Activation of plasminogen by tissue activator is increased specifically in the presence of certain soluble fibrin(ogen) fragments. *Thromb Res.* 1982;27(4):377-385.

(86) Schielen WJ, Voskuilen M, Tesser GI, Nieuwenhuizen W. The sequence A alpha-(148-160) in fibrin, but not in fibrinogen, is accessible to monoclonal antibodies. *Proc Natl Acad Sci U S A.* 1989;86(22):8951-8954.

(87) Lijnen HR, Bachmann F, Collen D et al. Mechanisms of plasminogen activation. *J Intern Med.* 1994;236(4):415-424.

(88) Zamarron C, Lijnen HR, Collen D. Kinetics of the activation of plasminogen by natural and recombinant tissue-type plasminogen activator. *J Biol Chem.* 1984;259(4):2080-2083.

(89) Holmer E, Kurachi K, Soderstrom G. The molecular-weight dependence of the rate-enhancing effect of heparin on the inhibition of thrombin, factor Xa, factor IXa, factor XIa, factor XIIa and kallikrein by antithrombin. *Biochem J.* 1981;193(2):395-400.

(90) Gyzander E, Teger-Nilsson AC. Activity of the alpha 2-macroglobulin-plasmin complex on the plasmin specific substrate H-D-Val-Leu-Lys-p-nitroanilide. *Thromb Res.* 1980;19(1-2):165-175.

(91) Barlow GH, Summaria L, Robbins KC. Molecular weight studies on human plasminogen and plasmin at the microgram level. *J Biol Chem.* 1969;244(5):1138-1141.

(92) Bouma BN, Marx PF, Mosnier LO, Meijers JC. Thrombin-activatable fibrinolysis inhibitor (TAFI, plasma procarboxypeptidase B, procarboxypeptidase R, procarboxypeptidase U). *Thromb Res.* 2001;101(5):329-354.

(93)   Van Walderveen MC, Berry LR, Atkinson HM, Chan AK. Covalent antithrombin-heparin effect on thrombin-thrombomodulin and activated protein C reaction with factor V/Va. *Thromb Haemost.* 2010;103(5):910-919.

(94)   Esmon CT. Protein C: biochemistry, physiology and clinical implications. *Blood.* 1983;62(6):1155-1158.